RAINFALL THRESHOLDS FOR THE INITIATION OF LANDSLIDES IN CENTRAL AND SOUTHERN EUROPE

Fausto Guzzetti, Silvia Peruccacci, Mauro Rossi
Istituto di Ricerca per la Protezione Idrogeologica, Consiglio Nazionale delle Ricerche, via Madonna Alta 126, 06128 Perugia, Italy

Colin P. Stark
Lamont-Doherty Earth Observatory, Columbia University, Route 9W, Palisades, NY 10964, USA

Summary

We review rainfall thresholds for the initiation of landslides world wide and propose new empirical rainfall thresholds for the Central European Adriatic Danubian South-Eastern Space (CADSES) area, located in central and southern Europe. One-hundred-twenty-four empirical thresholds linking measurements of the event and the antecedent rainfall conditions to the occurrence of landslides are considered. We then describe a database of 853 rainfall events that resulted or did not result in landslides in the CADSES area. Rainfall and landslide information in the database was obtained from the literature; climate information was obtained from the global climate dataset compiled by the Climate Research Unit of the East Anglia University. We plot the intensity-duration values in logarithmic coordinates, and we establish that with increased rainfall duration the minimum intensity likely to trigger slope failures decreases linearly, in the range of durations from 20 minutes to ~ 12 days. Based on this observation, we determine minimum intensity-duration (ID) and normalized-ID thresholds for the initiation of landslides in the CADSES area. Normalization is performed using two climatic indexes, the mean annual precipitation (MAP) and the rainy-day-normal (RDN). Threshold curves were inferred from the available data using a Bayesian statistical technique. Analysing the obtained thresholds we establish that lower average rainfall intensity is required to initiate landslides in an area with a mountain climate, than in an area characterized by a Mediterranean climate. We further suggest that for rainfall periods exceeding ~ 12 days landslides are triggered by factors not considered by the ID model. The obtained thresholds can be used in operation landslide warning systems, where more accurate local or regional thresholds are not available.

1. Introduction

Rainfall is a recognized trigger of landslides, and investigators have long attempted to determine the amount of precipitation needed to trigger slope failures, a problem of scientific and societal interest. Landslides triggered by rainfall are caused by the build up of water pressure into the ground (Campbell, 1975; Wilson, 1989). Groundwater conditions responsible for slope failures are related to rainfall through infiltration, soil characteristics, antecedent moisture content, and rainfall history (Wieczorek, 1996). These phenomena are poorly understood, and prediction of rainfall-induced landslides is problematic.

Here we review the literature on rainfall thresholds for the initiation of landslides, present a database of rainfall conditions that resulted or did not result in slope failures in the CADSES area and the neighbouring regions (Figure 1), and exploit this information to establish minimum intensity-duration and normalized intensity-duration thresholds for the occurrence of landslides in the CADSES area. We compare the new thresholds with existing thresholds in the study area and the neighbouring regions. We conclude discussing the results obtained, with emphasis on the possible application of the new thresholds in operational landslide warning systems.

2. Types and characteristics of rainfall thresholds

2.1 Definition of terms

A threshold is the minimum or maximum level of some quantity needed for a process to take place or a state to change (White et al., 1996). A minimum threshold defines the lowest level below which a process does not occur. A maximum threshold represents the level above which a process always occurs. For rainfall-induced landslides a threshold may define the rainfall, soil moisture, or hydrological conditions that, when reached or exceeded, are likely to trigger landslides. Rainfall thresholds can be defined on physical (process-based, conceptual) or empirical (historical, statistical) bases (Corominas, 2000; Crosta and Frattini, 2001; Aleotti, 2004; Wieczorek and Glade, 2005, and references therein).

2.2 Process-based models

Process-based models attempt to extend spatially the slope stability models (e.g. the “infinite slope model”) widely adopted in geotechnical engineering (Wu and Sidle, 1995; Iverson, 2000). To link rainfall pattern and history to slope stability/instability conditions, process-based models incorporate infiltration models (e.g., Green and Ampt, 1911; Philip, 1954; Salvucci and Entekabi,

1994). Various approaches have been proposed to predict the accumulation of the infiltrated water into the ground. Wilson (1989) proposed a "leaky barrel" model. In this model, a leaky barrel receives water from above at a given rate, and loses water from below at a different rate. The combination of recharge and leakage controls the accumulation of water and the build-up of pore water pressure that may cause slope instability. Wilson and Wieczorek (1995) used the leaky barrel model to forecast debris flow occurrence at La Honda, in the San Francisco Bay region. Crosta and Frattini (2003) compared three infiltration models, including a steady state model (Montgomery and Dietrich, 1994), a transient "piston-flow" model (Green and Ampt, 1911; Salvucci and Entekabi, 1994), and a transient diffusive model (Iverson, 2000), to predict the location and time of debris flows in the Lecco Province, in northern Italy.

Process-based models can determine the amount of precipitation needed to trigger slope failures, and the location and time of the expected landslides, making them of interest for landslide warning systems. However, limitations exist. Physical models require detailed spatial information on the hydrological, lithological, morphological, and soil characteristics that control the initiation of landslides. This information is difficult to collect precisely over large areas, and is rarely available outside specifically equipped test fields. Process-based models are calibrated using rainfall events for which precipitation measurements and the location and the time of slope failures are known. This information is not commonly available and is costly to obtain. Finally, physically based models perform best when attempting to predict shallow landslides (soil slides and debris flows), but are less efficient in predicting deep-seated landslides.

Crozier and Eyles (1980), Crozier (1999) and Glade et al. (2000) attempted a different approach to link soil moisture conditions to the occurrence (or lack of occurrence) of landslides. These authors developed an antecedent soil water status (ASWS) model, a simplified conceptual model that estimates soil moisture on a daily basis. The ASWS model performs a soil water balance that includes a drainage factor to account for the excess precipitation over a period of days prior to the day of the landslide event. The decay function for the loss of water through drainage and evapotranspiration is obtained, e.g., by analysing hydrograph recession curves (Glade et al., 2000). Crozier (1999) calibrated the ASWS model in the Wellington area, New Zealand, using rainfall and landslide information obtained for a severe landslide event occurred in 1974, and successfully predicted days with landslides and days without landslides for an 8-month period in 1996. Despite its proven capability, the model has not been implemented in a landslide warning system (Wieczorek and Glade, 2005).

2.3 Empirically based models

Empirical rainfall thresholds are defined by studying rainfall events that have resulted in landslides. The thresholds are usually obtained by drawing lower-bound lines to the rainfall conditions that resulted in landslides plotted in Cartesian, semi-logarithmic, or logarithmic coordinates. Most commonly, the thresholds are drawn visually, i.e., without any rigorous mathematical, statistical, or physical criterion. Where information on rainfall conditions that did not result in slope failures is available (e.g., Onodera et al., 1974; Lumb, 1975; Tatizana et al., 1987; Jibson, 1989; Corominas and Moya, 1999; Biafiore et al., 2002; Marchi et al., 2002; Zezere and Rodriquez, 2002; Pedrozzi, 2004; Giannecchini, 2005), thresholds are defined as the best separators of rainfall conditions that resulted and did not result in slope instability. The number of the triggered slope failures (e.g., single vs. multiple, first vs. abundant) can also be considered to construct a threshold.

Review of the literature (e.g., Wieczorek and Glade, 2005, and references therein) reveals that no unique set of measurements exists to characterize the rainfall conditions that are likely (or not likely) to trigger slope failures. Table 1 lists 25 rainfall and climate variables used in the literature for the definition of empirical thresholds for the initiation of landslides. Language inconsistencies and disagreement on the requisite rainfall and landslide variables make it difficult to compare the thresholds.

Key to the construction of empirical model to forecast the possible occurrence of rainfall-induced landslides is the definition of rainfall intensity. Rainfall intensity is the amount of precipitation accumulated in a period, or the rate of precipitation in a period, most commonly measured in millimetres (or inches) per hour. Depending on the length of the observation period, rainfall intensity may represent an “instantaneous” measure of the rainfall rate, or an average value of precipitation over hours (hourly intensity), days (daily intensity), or longer periods. For long observation periods, rainfall intensity represents an “average” value that underestimates the peak (maximum) rainfall rate occurred during the observation period. Hence, rainfall intensity measured over short and long periods have different physical meaning. This complicates the definition of rainfall models spanning a range of rainfall durations based on rainfall intensity. The majority of the intensity values used in this study are mean rainfall rates and not peak intensities.

Empirical thresholds for the initiation of landslides can be loosely defined as global, regional, or local thresholds. A global threshold attempts to establish a general (“universal”) minimum level below which landslides do not occur, independently of local morphological, lithological and land-use conditions and of local or regional rainfall pattern and history. Global thresholds have been

proposed by Caine (1980), Innes (1983), Jibson (1989), Clarizia et al. (1996), Crosta and Frattini (2001), and Cannon and Gartner (2005) (Tables 2, 3, 5, 6). Regional thresholds are defined for areas extending from a few to several thousand square kilometres of similar meteorological, climatic, and physiographic characteristics (Tables 2 to 6), and are potentially suited for landslide warning systems based on quantitative spatial rainfall forecasts, estimates, or measurements. Local thresholds explicitly or implicitly consider the local climatic regime and geomorphological setting, and are applicable to single landslides or to group of landslides in areas extending from a few to some hundreds of square kilometres (Tables 2 to 6). Regional and local thresholds perform reasonably well in the area where they were developed, but cannot be easily exported to neighbouring areas (Crosta, 1989). Global thresholds are relevant where local or regional thresholds are not available, but may result in (locally numerous) false positives, i.e. prediction of landslides that do not occur.

Based on the considered rainfall measurements, empirical rainfall thresholds can be further grouped in three broad categories: (i) thresholds that combine precipitation measurements obtained for a specific rainfall event, (ii) thresholds that consider the antecedent conditions, and (iii) other thresholds.

2.4 Thresholds that use event rainfall measurements

Thresholds using combinations of precipitation measurements obtained from individual or multiple rainfall events that resulted (or did not result) in landslides can be further subdivided in four sub-categories: (i) intensity – duration (ID) thresholds, (ii) thresholds based on the total event rainfall, (iii) rainfall event – duration (ED) thresholds, and (iv) rainfall event – intensity (EI) thresholds.

Intensity-duration thresholds are the most common type of thresholds proposed in the literature (52 thresholds listed in Table 2). Inspection of the Table 2 reveals that ID thresholds have the general form:

$$I = c + \alpha D^{\beta} \qquad (1)$$

where: I (mean) rainfall intensity, D is rainfall duration, and $c \geq 0$, α, and β are parameters.

The proposed ID thresholds span a considerable range of rainfall durations and intensities, but most of the thresholds cover the range of durations between 1 and 100 hr, and the range of intensities from 1 to 200 mm/h (Figure 2). For the majority of the ID thresholds (45 thresholds) $c = 0$. When $c = 0$ equation (1) is a simple power law. In Table 2, all the listed power laws have a negative scaling

exponents (β in the range between -1.50 and -0.19), and parameter α in the range from 4.00 to 176.40. The negative power law relation holds for four orders of magnitude of rainfall duration, suggesting a self-similar scaling behaviour of the rainfall conditions that result in landslides. However, the simple scaling behaviour has a conceptual limitation: for very long periods (e.g., D > 500 hours) even extremely small average rainfall intensities may result in landslides, a condition difficult to justify. This is partly a result of the different hydrological and slope stability significance of rainfall intensity different rainfall durations. To overcome this limitation, a few authors (e.g., Cannon and Ellen, 1985; Wieczorek, 1987; Crosta and Frattini, 2001) have proposed asymptotic thresholds for long rainfall durations. In Table 2, the asymptotic thresholds (#4, #5, #6, #34, #49) have β = -1.00 or -2.00 and c, the asymptotic (minimum) value of rainfall intensity for long rainfall durations, in the range from 0.48 to 6.90 mm/h. Three thresholds listed in Table 2 (#7, #9, #10) have β = 1.00 and c in the range from 49.11 to 92.06. These thresholds exhibit an asymptotic behaviour for very short rainfall durations.

Inspection of Figure 2 suggests the following generalizations. With the exception of the thresholds proposed by Caine (1980) (#1, determined with only 73 events worldwide) and by Jibson (1989) (#5, established as the lower envelope of eight ID thresholds determined for seven areas worldwide), global thresholds are positioned in the lower part of the ensemble of the ID thresholds. For rainfall durations in the range between 20 minutes and 5 hours, only two thresholds (#22, a local threshold for lahars in the Philippines, and #37, a regional threshold for shallow landslides in British Columbia) predict lower values of the average rainfall intensity likely to trigger slope failures. We attribute the lower level of rainfall intensity predicted by the global thresholds to their worldwide nature. By definition, global thresholds represent lowest levels below which rainfall-induced landslides should not occur.

Analysis of Figure 2 reveals that local thresholds are slightly higher than the regional thresholds, and higher than the global thresholds. This implies that, in general, local thresholds predict the initiation of rainfall induced landslides for slightly higher (or higher) average rainfall intensity for any given rainfall duration than the regional and the global thresholds. Local thresholds are generally defined for more limited ranges of rainfall duration, when compared to the regional and global thresholds. We attribute the observed differences primarily to an artefact introduced by the different geographical scales, which affect the rainfall sampling resolution. At the large (coarse) scale, measures of rainfall intensity are affected by regional averaging. Rainfall intensity augments

(systematically or stochastically) as the sampling resolution increases, resulting in more severe – but more realistic – ID conditions that initiate slope failures.

Further analysis of Figure 2 reveals differences in the thresholds proposed for similar and even for the same geographical areas. The regional threshold proposed by Guadagno (1991) (#16) for debris slides and debris flows in pyroclastic soils mantling carbonate rocks near Mt. Vesuvius (Campania region) is higher and steeper than the threshold proposed by Calcaterra et al. (2000) (#31) for all landslide types for the same region. Similarly, the thresholds proposed by Paronuzzi et al. (1998) (#24) for debris flows and by Marchi et al. (2002) (#35) for all landslide types in NE Italy are significantly different. Dissimilar are also the thresholds proposed by Arboleda and Martinez (1996) (#20) and Tuñgol and Regalado (1996) (#22) for the triggering of lahars in the Philippines. Identifying the reasons for the observed differences is difficult, as they may depend on the inherent variability of the rainfall conditions, on physiographical, geological or geomorphological differences, and on incompleteness in the rainfall and landslide data used to determine the thresholds.

A limitation of regional and local ID thresholds is the fact that thresholds defined for a specific region or area cannot be easily exported to neighbouring regions or similar areas (Crosta, 1989). In addition to morphological and lithological differences, this is due to meteorological (Jakob and Weatherly, 2003) and climate variability, which is not considered in the ID thresholds determined by studying individual rainfall events. To render comparable rainfall thresholds prepared for different areas or regions, investigators normalize the rainfall intensity values using empirical measures of the local climate. Most commonly, normalization is obtained dividing the event rainfall intensity by the mean annual precipitation (MAP) (e.g., Cannon, 1988; Jibson, 1989; Ceriani et al., 1992; Paronuzzi et al., 1998; Wieczorek et al., 2000; Aleotti et al., 2002; Bacchini and Zannoni, 2003). To normalize rainfall intensity, Wilson (1997) and Wilson and Jayko (1997) used the rainy-day normal (RDN), a climatic index that provides a better description (or proxy) than the MAP for the occurrence of extreme storm events most likely to trigger slope failures. Barbero et al. (2004) used the ratio between the MAP of two different areas (N) to export an ID threshold defined for the first area and to apply it to the second area.

Table 3 lists normalized ID thresholds proposed in the literature, and Figure 3 portrays the listed thresholds. With the exception of three thresholds (#53, #54, #56), all the normalized ID thresholds are represented by power laws, with scaling exponents β in the range from -0.79 to -0.21, and parameters α in the range from 0.02 to 4.62. Inspection of Figure 3 reveals two distinct groups of

thresholds, and a reduced variability of the gradient of the normalized thresholds, when compared to the ID thresholds shown in Figure 2. The reduced variability can be the result of normalization, but can also be spurious (i.e., due to the small number of the considered thresholds) or attributed to physiographical similarities between the regions for which the shown thresholds were prepared (e.g., nine thresholds are for areas in northern Italy, and 3 thresholds are for California). Despite normalization, in Figure 3 significant differences remain for local and regional thresholds defined for neighbouring or similar areas (e.g., #62 and #69 vs. #63). This may be the result of incompleteness or lack of homogeneity in the datasets used to define the thresholds, but also suggests geographic variability of the rainfall conditions likely to trigger landslides.

A few authors have attempted to establish thresholds for the initiation of landslides based on the amount of precipitation during the landslide triggering event (Table 4). Different rainfall variables have been used to define these thresholds, including: (i) daily rainfall (R), (ii) antecedent rainfall ($A_{(d)}$); (iii) cumulative event rainfall (E); and (iv) normalized cumulative event rainfall (E_{MAP}), often expressed as a percentage of the MAP. According to the last type of thresholds, if the total precipitation during a rainfall event exceeds an established percentage of the MAP, landslides are likely to occur, or to occur abundantly. As an example, Guidicini and Iwasa (1977), working in Brazil, determined that when the total event rainfall exceeded 12% of the MAP landslides were likely to occur independently of the antecedent conditions, whereas when the total event rainfall ranged from 8% to 12% of the MAP landslides initiation was dependant on rainfall history (#78). Similarly, Govi and Sorzana (1980), working in the Piedmont region of NW Italy, determined a relationship between the proportion of the MAP falling during a rainfall event and the abundance of the triggered landslides (#79), and discovered that areas characterized by large MAP required a larger amount of rainfall to trigger slope failures than areas characterized by low MAP. The normalized cumulative event rainfall (E_{MAP}) was also used by Bhandari et al. (1991) for E Himalayas (#83), and by Biafiore et al. (2002) for the KwaZulu-Natal province in South Africa (#89).

Other investigators have related the duration of the rainfall event (D) to measures of the event precipitation, including the cumulative event rainfall, the critical rainfall, and the corresponding normalized variables. Table 5 lists event – duration (ED) and normalized ED thresholds, and Figure 4 portrays the ED thresholds. The shown thresholds have similar ascending trends and exhibit comparable fixed or changing gradients, but differ significantly in the minimum amount of rainfall

required to trigger landslides (from 0.5 mm to more than 100 mm, for D = 1 hr). We attribute this to different climates in the considered regions.

Still other investigators have linked measures of the event rainfall to the average rainfall intensity, obtaining event–intensity (EI) and normalized EI thresholds (Table 6). Onodera et al. (1974), who were probably the first to propose quantitative rainfall thresholds for the initiation of landslides, further proposed a set of thresholds linking the hourly event intensity to the ratio between the average and the maximum rainfall intensity per hour. Govi and Sorzana (1980) adopted a slightly different approach and linked the average event rainfall during the final phase of the storm (i.e., the period when landslides occurred) to the critical event rainfall, normalized to the MAP. These authors found linear (in Cartesian coordinates) and complex relationships, depending on landslide abundance, on the season of the event, and on the antecedent rainfall conditions.

2.5 Thresholds that consider the antecedent conditions

Groundwater levels and soil moisture conditions are factors that predispose slopes to failure (Crozier, 1986; Wieczorek, 1996). The geographical pattern and temporal evolution of groundwater and soil moisture are difficult to know precisely, as they depend on various changing factors, including rainfall and temperature pattern and history. Antecedent precipitation influences groundwater levels and soil moisture, and can be used to determine when landslides are likely to occur.

A simple way of using antecedent precipitation measurements consists of establishing a threshold based on the amount of the antecedent rainfall. Govi et al. (1985) determined that the 60-day antecedent rainfall needed to trigger landslides in Piedmont region varied seasonally with a minimum value of 140 mm, and that the total precipitation (i.e., antecedent and event rainfall) needed to initiate slope failures was at least 300 mm. Cardinali et al. (2005) established that landslides in SW Umbria, central Italy, are likely to occur when antecedent rainfall exceeds 590 mm over a 3-month period, or 700 mm over a 4-month period.

More complex relationships between the antecedent precipitation and the event rainfall have been proposed. Terlien (1998), working in Colombia, related the normalized daily rainfall to the normalized antecedent rainfall. Pasuto and Silvano (1989), working in NE Italy, examined antecedent rainfall for different periods and the 2-day event rainfall (E_{2d}), and related them to the occurrence of past landslide events. These authors established that when the 15-day antecedent rainfall (A_{15d}) exceeded 200 mm the abundance of landslides in the Cordevole River basin

depended on the 2-day event rainfall. When E_{2d} exceeded 200 mm, landslides always occurred; for E_{2d} in the range from 100 and 150 mm, landslides occurred 57% of the time; and when E_{2d} was less than 70 mm, landslides occurred rarely. Kim et al. (1991), working in Korea, related the cumulative rainfall for a 3-day period before the landslide triggering event to the total daily rainfall for the day of the slope failure, and determined that landslides in central South Korea were influenced by the antecedent precipitation, whereas landslides in southern South Korea were controlled by the amount and intensity of the daily rainfall. De Vita (2000), working in southern Italy, also related the total daily rainfall for the day of the landslide to the antecedent rainfall, for periods from 1 to 60 days. This author established that for antecedent precipitation in the range between 1 and 19 days before the landslide event, the daily rainfall needed to trigger landslides decreased with the amount of the antecedent precipitation. If longer periods were considered, the daily rainfall required to initiate landslides first decreased and then levelled at about 50 mm. Chleborad (2003), working in the Seattle area, established a rainfall threshold to predict days with three or more landslides based on two precipitation measurements: the 3-day antecedent rainfall (i.e., the event rainfall), and the total rainfall for the 15-day period before the 3-day event rainfall (i.e., the antecedent rainfall). Heyerdahl et al. (2003), working in Nicaragua and El Salvador, defined a threshold for the triggering of lahars based on the critical hourly rainfall at failure and the antecedent precipitation for a 4-day period. For the Piedmont Region, Aleotti (2004) defined landslide initiation thresholds based on the normalized critical rainfall and the 7- and 10-day normalized antecedent rainfall. Gabet et al. (2004), working in the Himalayas, determined an empirical threshold for the triggering of landslides based on the daily rainfall and the accumulated monsoon rain. These authors further determined that a minimum seasonal antecedent rainfall of 528 mm must accumulate and a minimum daily rainfall of 9 mm must be exceeded before landslides are triggered in the Himalayas.

When using antecedent rainfall measurements to predict landslide occurrence, a key difficulty is the definition of the period over which to accumulate the precipitation. Review of the literature reveals a significant scatter in the considered periods. Kim et al. (1991) considered 3 days, Heyerdahl et al. (2003) considered 4 days, Crozier (1999) and Glade et al. (2000) considered 10 days, Aleotti (2004) selected 7, 10 and 15 days, and Chleborad (2003) used 18 days (3-day event rainfall and 15-day antecedent rainfall). Terlien (1998) tested 2-, 5-, 15- and 25-day periods and found best results for the longest rainfall periods. De Vita (2000) used antecedent periods from 1 to 59 days. Pasuto and Silvano (1989) tested rainfall periods from 1 to 120 days, and found best correlation with landslide occurrence for the 15-day antecedent rainfall. Cardinali et al. (2005) found a correlation between

landslide occurrence and the 3-month and the 4-month antecedent rainfall. This large variability can be attributed to different factors, including: (i) diverse lithological, morphological, vegetation and soil conditions, (ii) different climatic regimes and meteorological circumstances leading to slope instability, (iii) and heterogeneity and incompleteness in the rainfall and landslide data used to determine the thresholds.

A few authors have challenged the importance of the antecedent precipitation for the initiation of landslides. Aleotti (2004) did not find a correlation between the critical and the cumulative rainfall and the occurrence of landslides in the Piedmont region, NW Italy. Brand et al. (1984) did not find a correlation between the antecedent rainfall and the occurrence of slope failures in Hong Kong. This was explained by the very high rainfall intensity in tropical areas. Corominas and Moya (1999), working in the Pyrenees, observed that slopes covered by coarse debris exhibiting large interparticle voids were likely to generate debris flows without any significant antecedent precipitation. Similarly, Corominas (2000), considered possible the initiation of shallow landslides on slope mantled by impervious soils irrespective of the antecedent rainfall conditions, due to the presence of large macropores.

2.6 Other thresholds

A few other thresholds for the initiation of landslides have been proposed. Ayalew (1999) determined that the likelihood of slope failures in the Ethiopian Plateau was related to the product of two ratios: the number of days with rainfall exceeding 5 mm before the landslide event divided by RDs (a measure of evapotranspiration), and the cumulative rainfall up to the date of the landslide event divided by the MAP (a proxy for the effect of rainfall duration on soil water content). Wilson (2000) related the peak 24-hour rainfall amount from storms that triggered debris flows in California, Oregon, Washington, Hawaii and Puerto Rico to the maximum 24-hour rainfall expected in a 5-year return period. Wilson (2000) further proposed that the probability of debris flow occurrence was a function of the daily rainfall, normalized by the 5-year storm rainfall, indicating a climatic influence on the rainfall amount that is likely to initiate debris flows. Reichenbach et al. (1998) analysed historical mean daily discharge records for various gauging stations in the Tiber River basin, in central Italy, and related the discharge measurements to the occurrence (or lack of occurrence) of landslides. Relevant relationships were established for the flood volume and the maximum mean daily discharge, and for the event intensity and the maximum mean daily discharge. Jakob and Weatherly (2003) established hydroclimatic thresholds for the occurrence of slope failures in the North Shore Mountains of Vancouver, BC. Discriminant analysis of multiple

hydrological and rainfall variables selected (i) the number of hours discharge at a representative gauging station exceeded 1 m^3sec^{-1}, (ii) the 4-week cumulative rainfall prior to the storm (A_{28d}), and (iii) the maximum 6-hour cumulative event rainfall (E_{6h}) as the best predictors of landslide occurrence. Based on the three selected variables, Jakob and Weatherly (2003) established warning and initiation thresholds for debris flows and shallow landslides.

3. Database of rainfall and landslide events for the CADSES area

To determine rainfall thresholds for the occurrence of landslides in the CADSES area, we compiled a database of rainfall events that resulted (or did not result) in landslides in the study area and the neighbouring regions (Figure 1). The rainfall and landslide information was obtained from the literature, including international journals, conference proceedings, and reports describing single or multiple rainfall-induced landslide events. The obtained database lists 853 events collectively covering the period between 1841 and 2002, with the majority of the events in the period from 1954 to 2002. For each event, the collected information includes: (i) location of the area affected by the rainfall and the landslide event, (ii) rainfall conditions that resulted (or did not result) in the slope failures, (iii) type and number of the triggered landslides, (iv) main rock types cropping out in the region, and (v) climate information. Not all the information is available for all the events. Figure 5 summarises the type and amount of the available information.

Precise geographical information is available for 277 (32.5%) events (Figure 5A). For these events the site, village, town, or affected municipality is known. Of the remaining 576 events, 301 events (32.1%) were located with an intermediate level of precision (i.e., the province or the affected valley is known), and 274 events (32.1%) were attributed a low geographical precision (e.g., only the region, major valley, or general area is known). For one event only the nation was reported; we attributed to this event a very low geographical precision.

Rainfall information in the database includes: (i) intensity and duration of the rainfall event that resulted (or did not result) in landslides, (ii) cumulative amount of precipitation for the event, and (iii) measures of the antecedent precipitation. Information on rainfall intensity and duration is available for all the listed events, of which 663 (77.7%) resulted in landslides and 190 (22.3%) did not result in known slope failures (Figure 5B). Exact values or estimates of the total event precipitation are also available for all the rainfall events, whereas information on the antecedent precipitation is available for 38 events, 4.5% of the total (Figure 5C).

Significance of the rainfall intensity values listed in the database varies. For many of the short duration events ($D \leq 24$ hours), intensity was obtained directly from (sub-)hourly rainfall records. For several of the long and very long duration events ($D > 100$ hours) rainfall intensity was obtained dividing the accumulated event rainfall (E) by the rainfall duration (D). For the former events intensity represents the peak precipitation rate measured during the event, whereas for the latter events intensity represents an average estimate of the precipitation rate during the event.

Uncertainty exists in the rainfall information stored in the database. Some of the reports used to compile the database listed precise rainfall intensity and duration values. Most commonly, these reports were aimed at establishing local or regional rainfall thresholds for the initiation of slope failures. Reports aimed at describing single or multiple rainfall-induced landslides listed rainfall intensity and duration values, often without a precise description of how the information was obtained. For some of these reports, rainfall intensity and duration were average values, or estimates. Several reports showed graphs portraying the event rainfall history and the precise or approximate time or period of occurrence of the slope failures. From these reports, we obtained cumulative rainfall, rainfall intensity, and rainfall duration from the published graphs. Due to lack of standards for reporting rainfall intensity and antecedent rainfall conditions, inconsistency exists in the database for the measures of the rainfall intensity and the antecedent precipitations which preceded documented landslide events.

Landslide information in the database comprises: (i) type and depth of the slope movement, (ii) number of the triggered slope failures, and (iii) time, date or period of occurrence of the landslides. Landslides were classified as shallow (615, 92.8%), deep-seated (2, 0.3%), and of unknown depth (46, 6.9%). Shallow landslides were further subdivided into soil slips, debris flows, and unclassified shallow failures (Figure 5D). Classification was based primarily on the description of the landslides given in the reports, and subordinately on the type of failure (e.g., a soil slip was classified a shallow failure, and a large slide-earth flow was classified deep-seated). Only a few reports provided an exact number of the triggered failures. When the precise number was not available, a qualitative estimate was used, based on the information given in the reports (Figure 5E). For most of the events in the database (456, 68.8%) no information is available on the date or the time of occurrence of the slope failures (Figure 5F). The exact or approximate time of failure is known for 21 events (3.2%), and the date of the event is known for 112 events (16.9%). Landslide information also has uncertainty, which is largest for the number of the triggered landslides, and significant for the timing of the slope failures. The latter has many causes, including: the difficulty of establishing

the exact time of a landslide (landslides may occur during the night or in remote areas), and the fact that landslides may occur in pulses, during a period of time, or as reactivations of other landslides. Reporting also affects uncertainty, including the fact that single or multiple slope failures may be reported days or even weeks after they have occurred.

Information on lithology in the database consists of a generic description of the main rock types (e.g., sedimentary, intrusive, metamorphic rocks) cropping out in the area where landslides were triggered by rainfall. The lithological information was obtained from the literature or inferred from small-scale geological maps, and is available for 58.3% of the events listed in the database (Figure 5G).

Climate information is available for all rainfall events in the database. Each event was assigned to a class of the Köppen climate classification system, based on the geographical location of the area affected by the event. The majority of the listed events occurred in areas characterized by highland (i.e., mountain) climate, including the Alps (594 events, 69.6%), and in areas characterized by mild mid-latitude climates, including the Mediterranean climate (250 events, 29.3%) (Figure 5H). Values for the MAP and the RDs were obtained from the grid data in the Global Climate Dataset compiled by the Climate Research Unit (CRU) of the East Anglia University, available through the Data Distribution Centre of the Intergovernmental Panel on Climate Change (IPCC). The CRU dataset consists of a suite of surface climate variables obtained by interpolating a large number of meteorological stations, including 19,800 rainfall stations worldwide. In the dataset, climate data are available for all land masses, excluding Antarctica, on a grid of 0.5° latitude by 0.5° longitude resolution (approximately 40 km N by 40 km E at mid latitudes), and cover systematically the 30-year period from 1961 to 1990 (New et al., 1999). Based on this climate information, rainfall events listed in the database occurred in areas with between 135 and 230 rainy-days (Figure 5I), and MAP in the range from 600 to 2000 mm, with the majority of the events occurring in areas having MAP in the range between 1300 and 1600 mm (Figure 5J).

4. Rainfall thresholds for the CADSES area

We used the rainfall, landslide and climate information stored in the database to determine rainfall thresholds for the initiation of landslides in the CADSES area. We defined intensity-duration (ID) thresholds and normalized-ID thresholds, and we performed the analysis on the entire set of ID data, and on two climatic subsets.

4.1 Intensity – duration thresholds

We started by plotting all the available ID data in a single graph (Figure 6A). In this ID plot, rainfall conditions that resulted in landslides (663 events) are shown by filled symbols, and rainfall conditions that did not result in slope failures (190 events) are shown by open circles. The majority of the rainfall events with landslides have duration in the range between 1 and 200 hours, and rainfall intensity in the range between 0.05 and 30 mm/hour. Figure 6A reveals clustering of the reported events at specific durations (e.g., D = 0.5, 1, 2, 3, 6, 12, 24, 48 and 72 hours). This outlines a bias in the database, due to the availability of rainfall measurements for pre-defined recording periods. Despite considerable scattering and clustering at specific durations, a clear trend exists in the ID data. With increased rainfall duration, the minimum intensity likely to trigger slope failures decreases linearly in the log-log plot. The self-similar behaviour is clear for at least three orders of magnitude of rainfall duration, i.e., from less than 20 minutes to about 12 days.

Next, starting from the ID data shown in Figure 6A we obtained the probability graph portrayed in Figure 6B. In this graph, for any specific rainfall duration, each line shows the probability that a percentage of the known landslide events (filled symbols in Figure 6A) lays below the line. As an example, for any rainfall duration, 2% of the landslide events were triggered by rainfall intensity lower than the intensity shown by the lowest line in the graph, and 5% of the events were triggered by rainfall intensity lower than the intensity shown by the second lowest line in the graph. To minimize the effect of clustering at specific durations, and to estimates values at empty logarithmic bins, we adopted a moving-average filtering technique. At each logarithmic bin along the duration axis (x-axis) we centred a moving window, 5 logarithmic bins in width (i.e., two bins to the left and two bins the right of the central bin). We selected all the data points in the 5-bin moving window, and we computed the percentiles along the intensity axis, from the 2nd to the 95th percentile. We attributed the computed percentiles of rainfall intensity to the central point of the moving window along the duration axis. Next, the moving window was shifted one logarithmic bin along the x-axis, and the calculation was repeated. Probability lines were then drawn by joining equal percentile points. To construct the probability plots we discarded 3 points having $D \sim 30$ minutes and $I \sim 3$ mm/h. These points, obtained from Crosta and Frattini (2001) and Bacchini and Zannoni (2003), do not fit the linear trend for the minimum intensity likely to trigger landslides shown by the other data, and were considered outliers.

Inspection of Figure 6B confirms the linear scaling of the minimum level (i.e., 2nd percentile line) of rainfall intensity likely to trigger landslides in the range of duration from about 20 minutes to

about 200 hours (~ 8 days). For longer durations, the probability plot shows more clearly than the original ID data the break in the linear behaviour. When rainfall duration exceeds about 100 hours, an average rainfall intensity exceeding 0.20 mm/h is likely to trigger landslides independently of rainfall duration.

A Bayesian approach was used to define a threshold model for likely landslide occurrence and to permit its calibration in a reasonably objective fashion. From eq. (1), a threshold curve of the form $I = \alpha D^{-\beta}$ was chosen to generalize the shape of the threshold, i.e. a power law with a negative scaling exponent β. A probability approach was then used to find the scale α and the shape β of the curve. This was achieved by defining a Bernoulli "coin toss" probability of a landslide data point occurring at a given value of I and D:

$$P(I, D) \sim dbern[\mu(I, D)] \qquad (2)$$

This probability variable, which takes a value of 0 or 1, expresses the combined chances of (i) storm incidence with peak intensity I and duration D, (ii) consequent landslide failure, and (iii) subsequent observation and reporting of the landslide event. The model function

$$\mu(I, D) = \{(1-\delta)\,\Theta[z(I, D)] + \delta\} \exp[-\eta|z(I, D)|] \qquad (3)$$

where Θ is the Heaviside step function (Abramowitz and Stegun, 1972, p. 1020), describes the zone of likely landslide observations (Figure 6A) centred along a quasi-hyperbolic (negative power-law) axis set by the function

$$z(I, D) = 1 - \alpha \left(I\, D^{\beta}\right)^{-1} \qquad (4)$$

The parameters δ and η together represent both the spread of data points across the I-D plane (Figure 6B) and the "smear" of data points across the inferred threshold along z (Figures 6C). The model was designed so that a probability distribution of possible threshold curves, loosely defining the boundary of the point data cloud, could be estimated. After some experimentation with model inference, the tolerance values were set to $\delta = 0.1$ and $\eta = 0.5$, while prior probability distributions for α and ß were chosen at:

$$1/\alpha \sim dunif[0.1, 100] \qquad (5a)$$

$$\beta \sim dunif[0.1, 2] \qquad (5b)$$

Estimated values of α and β were obtained through Bayesian inference of their posterior probability distributions given the model and the data. Inference was performed using a package called *WinBUGS* (http://www.mrc-bsu.cam.ac.uk/bugs/), using the "ones" trick to solve for Bernoulli probabilities with known outcomes (landslide occurrence).

We performed Bayesian inference on three different datasets. The first dataset consisted of 663 ID points that resulted in landslides, i.e., the filled symbols in Figure 6A. The second and the third datasets were obtained from the 2nd percentile estimates (dots in Figure 6B), and consisted of 653 points in the range of rainfall durations from 5 minutes to 700 hours, and of 18 points in the range of durations from 300 to 4000 hours, respectively. These two, partially overlapping, datasets were selected to study the change in the linear scaling of the minimum rainfall intensity needed to trigger landslides at durations of about 400 hours, i.e. where the self similar ID model begins to be inadequate to predict slope failures. Results are shown in Figure 6C. When the entire ensemble of the ID data is considered, the obtained minimum threshold for the possible initiation of landslides (grey line in Figure 6C) is slightly less steep but not much different than the threshold obtained from the estimated ID values taken along the 2nd percentile line, the latter for rainfall durations shorter than 700 hours. For rainfall duration exceeding 300 hours, the Bayesian analysis inferred a significantly different threshold, in better agreement with the (few) available data.

The minimum level of ID necessary to initiate landslides can also be well approximated by a single, asymptotic threshold curve with equation $I = 0.1 + 8.5D^{-0.65}$, obtained by linearly fitting ID points sampled along the thresholds curve obtained from the 2nd percentile estimates.

To test the performance of the obtained thresholds as lower-limit lines to the ID conditions that resulted in landslides, for each logarithmic bin along the duration axis we counted the number of the rainfall events that triggered landslides and that were below the ID thresholds (i.e., the false positives). As a working simplification, for each logarithmic bin we selected the lowest of the inferred thresholds. Results are shown in Figure 7A, and indicate that only a limited number of the know rainfall events that have generated landslides are located below the minimum ID thresholds.

4.2 Intensity – duration thresholds for different climatic regimes

To study the importance of climate in the definition of ID rainfall thresholds in the CADSES area, we subdivided the available rainfall events in two climatic groups, specifically: (i) group I, comprising 250 events (164 with landslides and 64 without landslides) that occurred in mild mid-latitude climates, including the Mediterranean climate, and (ii) group II, listing 603 events (499

with landslides and 104 without landslides) which occurred in mountain regions, including the Alps (393 events), in areas characterized by severe mid-latitude climate (6 events) and in Polar regions (3 events). Figures 8A and 8B show the climatically subdivided data, Figures 8C and 8D the corresponding percentiles plots, and Figures 8E and 8F the related threshold curves obtained through Bayesian inference. Figures 7B and 7C measure the performance of the established thresholds as lower-limit lines to the conditions that resulted in landslides in the climatically subdivided datasets.

Rainfall events pertaining to group I (Figure 8A) exhibit a reduced scatter and a distinct linear trend for the minimum level of rainfall intensity needed to trigger landslides, at least in the range of duration from about 1 to at least 200 hours. The percentiles plot (Figure 8C) confirms the linear trend for rainfall durations from 1 to 200 hours. For durations exceeding 600 hours, an average rainfall intensity of 0.20 mm/h appears to be sufficient to initiate landslides. In the intermediate range of rainfall durations (i.e., $200 < D < 600$ hours), the shape of the minimum threshold is less well constrained. For rainfall events in climate pertaining to group II (Figure 8B) the scatter in the ID data is larger, and the linear trend in the minimum values that have resulted in landslides is less distinct, but present in the range of durations from about 30 minutes to 200 hours. For longer rainfall periods, due to the scarcity of the data, the trend is poorly determined, but a minimum average intensity of 0.3 mm/h appears to be sufficient to initiate slope failures.

4.3 Normalized intensity – duration thresholds

To further investigate the minimum rainfall intensity required to trigger landslides in the CADSES area, we determined normalized-ID thresholds. For the purpose we exploited the MAP and RDs data obtained from the Global Climate Dataset compiled by the East Anglia University Climate Research Unit. Two normalizations were performed. The first normalization consisted of dividing the rainfall intensity by the MAP. The second normalization was performed by dividing the rainfall intensity by the RDN, a different proxy for climate than the MAP (Table 1). The normalized thresholds were obtained by adopting the same procedure described above for the non-normalized thresholds. First, the normalized ID data were plotted on I_{MAP}-D and I_{RDN}-D plots, for all the data and for the climatically subdivided subsets. Next, the corresponding percentile plots were prepared. Then, normalized-threshold models were inferred using the same Bayesian technique adopted before, adjusting the prior probability distributions for the size parameter α to the changed units of measures. Results are shown in Figure 9 for the two different normalizations and for the different datasets. Figures 7D-I summarize the performances of the normalized thresholds.

5. Discussion and concluding remarks

The new thresholds for the possible initiation of rainfall-induced landslides in the CADSES area were inferred from the available rainfall intensity and duration data using a Bayesian statistical approach, which maximized objectivity and reduced interpretation errors. This is an improvement over existing methods to determine empirical thresholds based on visual interpolation or curve fitting. The approach can be exported to other areas and applied to different datasets. In principle, the model can be expanded to consider different types of threshold curves.

Inspection of Figure 6 reveals the range of rainfall ID conditions likely to result in hill slope failures in the CADSES area. The considerable range of rainfall durations (from a few minutes to a few months) suggests different meteorological and hydrological conditions likely to initiate slope failures. Events characterized by high intensity and short rainfall duration (e.g., the result of convective thunderstorms) can trigger mostly shallow landslides and debris flows in relatively high permeability soils (Corominas and Moya, 1999; Colominas, 200). Long rainfall periods characterized by low to moderate average rainfall intensity (e.g. the result of multiple storms during a period of weeks or months) can initiate shallow and deep-seated landslides in low permeability soils and rocks (Cardinali et al., 2006).

Analysis of the ID data shown in Figure 6 reveals a clear descending trend of the minimum level of average rainfall intensity needed to initiate slope failures, with increasing rainfall duration. The linear trend is well approximated by the ID threshold curves for duration up to ~ 200 hours (~ 8 days). For longer rainfall periods the self similar behaviour of the ID data is less clear, and different interpretations of the lower limit curves are possible. This is partly due to the lack of data for long rainfall periods – a consequence of the incompleteness of the database – but it is also indication that, in the range of duration from 100 to 500 hours (~ 4 to ~ 21 days), variability (uncertainty) exists in the minimum average rainfall intensity required to trigger landslides. This is the range of durations for which the antecedent precipitation and soil moisture conditions are most important for the initiation of landslides (e.g., Pasuto and Silvano, 1989; Crozier, 1999; Glade et al., 2000; Chleborad, 2003; Jakob and Weatherly, 2003; Aleotti, 2004), and particularly to trigger slope failures in impervious, clay rich terrains. For long durations, evapotranspiration also becomes important. Due to evapotranspiration, a low average rainfall intensity results in an effective rainfall equal or close to zero. This suggests that slope failures triggered after long periods of low rainfall intensity are the result of processes not accounted for by the simple ID model adopted here (e.g. deep groundwater recharge, progressive rupture, etc.).

Comparison of the threshold curves obtained for the climatically subdivided datasets (Figure 8) reveals that the minimum levels of rainfall intensity likely to generate landslides in the two climatic subdivisions are different. Thresholds defined for mild mid-latitude climates (group I) are steeper ($0.70 < \beta < 0.81$) than the thresholds obtained for the mountain and cold climates (group II) ($0.48 < \beta < 0.64$). For the same short rainfall duration ($D < 30$ hour), a lower (average) rainfall intensity is required to initiate landslides in an area with a mountain climate, than in an area characterized by a mild mid-latitude climate. Conversely, for long rainfall periods, a lower (average) intensity is needed to trigger landslides in a mild mid-latitude climate area than in an area characterized by a mountain climate. In regions with a mild mid-latitude climate, rainfall duration is more important than rainfall intensity to trigger landslides, whereas in mountain areas intensity is more relevant than duration to initiate slope failures.

Comparison between the ID thresholds (Figures 6 and 8) and the normalized-ID thresholds (Figures 9) does not reveal large variations. The general trend of the threshold curves remains the same, and the shape of the thresholds is largely preserved. This was expected, as the two normalizations were essentially a re-scaling of the original ID data. However, differences exist in the determined thresholds. Normalization provides better agreement between the threshold curves inferred from the entire set of the ID data, and the curves inferred using the 2nd percentile estimates of the ID rainfall conditions, for duration not exceeding 300 hours. Normalization to the RDN performed slightly better than normalization to the MAP. Normalization also extended slightly the range of rainfall duration for which a linear trend is observed in the minimum average intensity required to initiate slope failures. Thus, for long rainfall periods, the normalized-ID data and the corresponding thresholds are somewhat less affected by the antecedent precipitation conditions. The two performed normalizations (to the MAP and to the RDN) have not captured entirely the existing meteorological variability of the considered climates. Different normalizations can be devised to (better) represent the observed annual rainfall variability in the considered climates. These normalizations may result in better comparable normalized-ID thresholds.

The new thresholds determined for the CADSES area can be compared with similar thresholds proposed in the literature for the same area and the neighbouring regions. Figure 10 shows the new thresholds obtained for the CADSES area using the entire set of rainfall events (thick grey lines), and compares them with (black lines): (i) global ID thresholds (1 to 5), (ii) regional and local thresholds for the CADSES area (6 to 11), and (iii) local thresholds for the neighbouring Piedmont Region, in NW Italy (12 to 18). The new thresholds are generally lower than local and regional

thresholds. We attribute this to the fact that the new thresholds were defined using rainfall and landslide data collected from different and distant areas, and cannot be considered regional or local thresholds. The relationship between the new thresholds and the global thresholds (1 to 5) is more difficult to interpret. The new thresholds are substantially lower than the threshold curve proposed by Jibson (1989). For short rainfall durations, the new thresholds are higher than the thresholds proposed by Caine (1980) and Innes (1983), but lower than the thresholds proposed by Clariza et al. (1996) and Crosta and Frattini (2001). For intermediate rainfall durations, our thresholds are lower than Caine's and Jibson (1989) thresholds, but higher than the other global thresholds. For long rainfall durations, the new thresholds are significantly lower than most of the other global thresholds. We further note that the minimum average rainfall intensity defined by Crosta and Frattini (2001) as necessary to initiate landslides for long rainfall periods ($D > 7$ days) is at least 3 times higher that the minimum average intensity identified by the new thresholds for corresponding durations.

Figure 10 also shows the range of the minimum intensity required to initiate landslides encompassed by the different thresholds inferred from the climatically subdivided data (Figure 8). The grey pattern in Figure 10 can be considered a proxy for the uncertainty in the definition of the new thresholds. This information may be useful in operational landslide warning systems.

Rainfall events resulting in landslides used to construct the new thresholds for the CADSES area produced different types of slope failures, but predominantly shallow failures, including soil slips and debris flows (Figure 5D). This information must be considered when using the thresholds in a landslide warning system. The new thresholds for the CADSES area should be intended as lower limit rainfall conditions that, when exceeded, are likely to trigger shallow landslides. The obtained thresholds can also be used to forecast the occurrence of deep-seated landslides, particularly after long rainfall periods, but with increased uncertainty.

In the CADSES area landslides occur every year, claiming lives and causing disruption. Empirical rainfall thresholds for the initiation of landslides may play a role in helping mitigating landslide risk (Aleotti, 2004; Wieczorek and Glade, 2005). Where local or regional thresholds have been determined, the thresholds can be used to predict the likely occurrence of slope failures in an area, provided rainfall measurements or quantitative precipitation forecasts are available. Landslide warning systems based on empirical rainfall thresholds and systematic rainfall measurements or forecasts, are – or have been – operational, e.g., in Hong Kong (Premchitt et al., 1994), the San Francisco Bay region (Keefer et al., 1987), Rio de Janeiro (D'Orsi et al., 1997), Nagasaki (Iwamoto,

1990), Jamaica (Ahmad, 2003), the Piedmont region (Aleotti, 2004), and the Yangtze River (International Early Warning Programme, 2005). Similar systems can be established for the CADSES area using local, regional or global thresholds.

Local and regional rainfall thresholds for the occurrence of landslides have been determined for a few places in the CADSES area (Figure 10). In these places the available thresholds can be used to establish local or regional landslide warning systems. However, for the majority of the CADSES area local or regional thresholds have not been defined, and the rainfall and landslide information needed to determine the thresholds is missing or costly to obtain. The new thresholds defined in this work can be used in the areas where thresholds are not available. When adopting the new thresholds to establish operational landslide warning systems, caution must be used as the thresholds were defined statistically, using a limited, geographically biased, and certainly incomplete dataset. Since the new thresholds are comparable to global thresholds, dependence of average rainfall intensity on the measuring spatial resolution should be carefully considered. The established thresholds are affected by uncertainty, and may result in "false positives", i.e., they may predict landslides that do not occur. Conversely, there is always a (small) probability of slope failures occurring with rainfall conditions below the threshold. Furthermore, landslides can be triggered by causes different than intense or prolonged rainfall. The new thresholds presented in this work will not predict landslides caused by snowmelt, earthquakes or human activity.

6. Acknowledgements

Research supported by RISKAWARE, a research project partly financed by the European Commission through the Interreg IIIB – CADSES programme. CPS was supported by NSF grant 0229846.

7. References

Abramowitz M, Stegun IA (1972) Handbook of Mathematical Functions with Formulas, Graphs, and Mathematical Tables. National Bureau of Standards, John Wiley and Sons, 10th edition, New York, 1046 pp

Ahmad R (2003) Developing early warning systems in Jamaica: rainfall thresholds for hydrological hazards. National Disaster Management Conference, Ocho Rios, St Ann, Jamaica, 9-10 September 2003. at website: http://www.mona.uwi.edu/uds/rainhazards_files/frame.htm

Aleotti P (2004) A warning system for rainfall-induced shallow failures. Eng Geol 73: 247–265

Aleotti P, Baldelli P, Bellardone G, Quaranta N, Tresso F, Troisi C, Zani A (2002) Soil slips triggered by October 13-16, 2000 flooding event in the Piedmont Region (North West Italy): critical analysis of rainfall data. Geologia Tecnica e Ambientale 1: 15–25

Annunziati A, Focardi A, Focardi P, Martello S, Vannocci P (2000) Analysis of the rainfall thresholds that induced debris flows in the area of Apuan Alps – Tuscany, Italy (19 June 1996 storm). In: Proceeding of the EGS Plinius Conference on Mediterranean Storms. Maratea, Italy, 485–493

Arboleda RA, Martinez ML (1996) 1992 lahars in the Pasig-Potrero River system. In: Fire and mud: eruptions and lahars of Mount Pinatubo (Newhall CG, Punongbayan RS, eds). Philippine Institute of Volcanology and Seismology, Quezon City and University of Washington Press, Seattle, 1126 pp

Ayalew L (1999) The effect of seasonal rainfall on landslides in the highlands of Ethiopia. Bull Eng Geol Env 58: 9–19

Bacchini M, Zannoni A (2003) Relations between rainfall and triggering of debris-flow: a case study of Cancia (Dolomites, Northeastern Italy). Nat Hazard Earth Sys 3: 71–79

Barbero S, Rabuffetti D, Zaccagnino M (2004) Una metodologia per la definizione delle soglie pluviometriche a supporto dell'emissione dell'allertamento. In: Proceedings 29th Convegno Nazionale di Idraulica e Costruzioni Idrauliche. Trento: 7-10 September 2004, 211–217

Baum RL, Godt JW, Harp EL, McKenna JP (2005) Early warning of landslides for rail traffic between Seattle and Everett, Washington. In: Landslide Risk Management, Proceedings of the 2005 International Conference on Landslide Risk Management (Hungr O, Fell R, Couture R, Ebdrhardt E, eds). New York: A.A. Balkema, 731–740

Bell FG, Maud RR (2000) Landslides associated with the colluvial soils overlying the Natal Group in the greater Durban region of Natal, South Africa. Environ Geol 39(9): 1029–1038

Bhandari RK (1984) Simple & economical instrumentation and warning systems for landslides & other mass movements. In: Proceedings 4th International Symposium on Landslides. Toronto, Canada, 1: 251–305

Bhandari RK, Senanayake KS, Thayalan N (1991) Pitfalls in the prediction on landslide through rainfall data. In: Landslides (Bell DH, ed). Rotterdam: A.A. Balkema, 2: 887–890

Biafiore M, Braca G, De Blasio A, Martone M, Onorati G, Tranfaglia G (2002) Il monitoraggio ambientale dei territori campani a rischio di frane e di alluvioni: lo sviluppo della rete idropluviometrica del Servizio Idrografico e Mareografico Nazionale. Unpublished report.

Bolley S, Oliaro P (1999) Analisi dei debris flows in alcuni bacini campione dell'Alta Val Susa. Geoingegneria Ambientale e Mineraria, Marzo: 69–74

Brand EW, Premchitt J, Phillipson HB (1984) Relationship between rainfall and landslides in Hong Kong. In: Proceedings 4th International Symposium on Landslides. Toronto: 1: 377–384

Caine N (1980) The rainfall intensity-duration control of shallow landslides and debris flows. Geogr Ann A 62: 23–27

Calcaterra D, Parise M, Palma B, Pelella L (2000) The influence of meteoric events in triggering shallow landslides in pyroclastic deposits of Campania, Italy. In: Proceedings 8th International Symposium on Landslides, (Bromhead E, Dixon N, Ibsen ML, eds). Cardiff: A.A. Balkema, 1: 209–214

Campbell RH (1975) Soil slips, debris flows, and rainstorms in the Santa Monica Mountains and vicinity, southern California. In: US Geological Survey Professional Paper 851. Washington DC: U.S. Government Printing Office, 51 pp

Cancelli A Nova R (1985) Landslides in soil debris cover triggered by rainstorms in Valtellina (central Alps - Italy). In: Proceedings 4th International Conference and Field Workshop on Landslides. Tokyo: The Japan Geological Society, 267–272

Cannon SH (1988) Regional rainfall-threshold conditions for abundant debris-flow activity. In: Landslides, Floods, and Marine Effects of the Etorm of January 3-5, 1982, in the San Francisco Bay Region, California (Ellen SD, Wieczorek GF, eds). US Geological Survey Professional Paper 1434, 35–42

Cannon SH, Ellen SD (1985) Rainfall conditions for abundant debris avalanches, San Francisco Bay region, California. Calif Geol 38: 267–272

Cannon SH, Gartner JE (2005) Wildfire-related debris flow from a hazards perspective. In: Debris flow Hazards and Related Phenomena (Jakob M, Hungr O, eds). Springer Berlin Heidelberg, 363–385

Canuti P, Focardi P, Garzonio CA (1985) Correlation between rainfall and landslides. Bull Int Assoc Eng Geol 32: 49–54

Cardinali M, Galli M, Guzzetti F, Ardizzone F, Reichenbach P, Bartoccini P (2005, submitted) Rainfall induced landslides in December 2004 in South-Western Umbria, Central Italy. Nat Hazard Earth Sys Sci 6: 237–260

Ceriani M, Lauzi S, Padovan N (1992) Rainfall and landslides in the Alpine area of Lombardia Region, central Alps, Italy. In: Interpraevent Int. Symposium. Bern: 2: 9–20

Chien-Yuan C, Tien-Chien C, Fan-Chieh Y, Wen-Hui Y, Chun-Chieh T (2005) Rainfall duration and debris-flow initiated studies for real-time monitoring. Environ Geol 47: 715–724

Chleborad AF (2003) Preliminary Evaluation of a Precipitation Threshold for Anticipating the Occurrence of Landslides in the Seattle, Washington, Area, US Geological Survey Open-File Report 03-463

Clarizia M, Gullà G, Sorbino G (1996) Sui meccanismi di innesco dei soil slip. In: International Conference Prevention of Hydrogeological Hazards: the Role of Scientific Research (Luino F ed.). Alba: L'Artistica Savigliano pub, 1: 585–597

Corominas J (2000) Landslides and climate. Keynote lecture- In: Proceedings 8th International Symposium on Landslides, (Bromhead E, Dixon N, Ibsen ML, eds). Cardiff: A.A. Balkema, 4: 1–33

Corominas J, Moya J (1996) Historical landslides in the Eastern Pyrenees and their relation to rainy events. In: Landslides (Chacon J, Irigaray C, Fernandez T, eds). Rotterdam: A.A. Balkema, 125–132

Corominas J, Moya J (1999) Reconstructing recent landslide activity in relation to rainfall in the Llobregat River basin, Eastern Pyrenees, Spain. Geomorphology 30: 79–93

Corominas J, Ayala FJ, Cendrero A, Chacón J, Díaz de Terán JR, Gonzáles A, Moja J, Vilaplana JM (2005) Impacts on natural hazard of climatic origin. In ECCE Final Report: A Preliminary Assessment of the Impacts in Spain due to the Effects of Climate Change. Ministerio de Medio Ambiente. http://www.mma.es/secciones/cambio_climatico/documentacion_cc/historicos_cc/pdf/preliminary_assessment_impacts_full_2.pdf

Crosta GB (1989) A study of slope movements caused by heavy rainfall in Valtellina (Italy - July 1987). In: Proceedings 6th International Conference and Field Workshop on Landslides ALPS 90 (Cancelli A, ed). Milano: Ricerca Scientifica ed Educazione Permanente, 79b: 247–258

Crosta GB, Frattini P (2001) Rainfall thresholds for triggering soil slips and debris flow. In: Proceedings 2nd EGS Plinius Conference on Mediterranean Storms (Mugnai A, Guzzetti F, Roth G, eds). Siena: 463–487

Crosta, GB, Frattini P (2003) Distributed modelling of shallow landslides triggered by intense rainfall. Nat Hazard Earth Sys Sci 3(1-2): 81–93

Crozier MJ (1986) Landslides: causes, consequences and environment. London: Croom Helm, 252 pp

Crozier MJ (1999) Prediction of rainfall-triggered landslides: a test of the antecedent water status model. Earth Surf Proc Land 24: 825–833

Crozier MJ, Eyles RJ (1980) Assessing the probability of rapid mass movement. In: Proceedings of 3rd Australia-New Zealand Conference on Geomechanics (Technical Groups, eds). Wellington: New Zealand Institution of Engineers, 6: 247–251

D'Orsi R, D'Avila C, Ortigao JAR, Dias A, Moraes L, Santos MD (1997) Rio-Watch: the Rio de Janeiro landslide watch system. In: Proceedings of the 2nd PSL Pan-AM Symposium on Landslides. Rio de Janerio, 1: 21–30

De Vita P (2000) Fenomeni di instabilità della coperture piroclastiche dei monti Lattari, di Sarno e di Salerno (Campania) ed analisi degli eventi pluviometrici determinanti. Quaderni di Geologia Applicata, 7(2): 213–235

Endo T (1970) Probable distribution of the amount of rainfall causing landslides. Annual report, Hokkaido Branch, Govern. Forest Experiment Station, Sapporo, 123–136.

Floris M, Mari M, Romeo RW, Gori U (2004) Modelling of landslide-triggering factors – A case study in the Northern Apennines, Italy. In: Lecture Notes in Earth Sciences 104: Engineering Geology for

Infrastructure Planning in Europe (Hack R, Azzam R, Charlier R, eds). Springer-Verlag Berlin Heidelberg, 745–753

Gabet EJ, Burbank DW, Putkonen JK, Pratt-Sitaula BA, Oiha T (2004) Rainfall thresholds for landsliding in the Himalayas of Nepal. Geomorphology 63: 131–143

Giannecchini R (2005) Rainfall triggering soil slips in the southern Apuane Alps (Tuscany, Italy). Adv Geosci 2: 21–24

Glade T, Crozier MJ, Smith P (2000) Applying probability determination to refine landslide-triggering rainfall thresholds using an empirical "Antecedent Daily Rainfall Model". Pure Appl Geophys, 157(6/8): 1059–1079

Govi M, Mortara G, Sorzana P (1985) Eventi idrologici e frane. Geologia Applicata & Ingegneria 20(2): 359–375

Govi M, Sorzana PF (1980) Landslide susceptibility as function of critical rainfall amount in Piedmont basin (North-Western Italy). Studia Geomorphologica Carpatho-Balcanica 14: 43–60

Green WH, Ampt G (1911) Studies of soil physics. Part I. The flow of air and water through soils. J Agr Sci 4: 1–24

Guadagno FM (1991) Debris flows in the Campanian volcaniclastic soil (Southern Italy). In: Proceedings International Conference on slope stability. Isle of Wight: Thomas Telford, 125–130

Guidicini G, Iwasa OY (1977) Tentative correlation between rainfall and landslides in a humid tropical environment. Bull Int Ass Eng Geol 16: 13–20

Heyerdahl H, Harbitz CB, Domaas U, Sandersen F, Tronstad K, Nowacki F, Engen A, Kjekstad O, Dévoli G, Buezo SG, Diaz MR, Hernandez W (2003) Rainfall induced lahars in volcanic debris in Nicaragua and El Salvador: practical mitigation. In: Proceedings of International Conference on Fast Slope Movements – Prediction and Prevention for risk Mitigation, IC-FSM2003. Naples: Patron Pub, 275–282

Hong Y, Hiura H, Shino K, Sassa K, Suemine A, Fukuoka H Wang G (2005) The influence of intense rainfall on the activity of large-scale crystalline schist landslides in Shikoku Island, Japan. Landslides 2(2): 97–105

Innes JL (1983) Debris flows. Prog Phys Geog 7: 469–501

Iverson RM (2000) Landslide triggering by rain infiltration. Water Resour Res 36(7): 1897–1910

Iwamoto M (1990) Standard amount of rainfall for warning from debris disaster. In: Proceedings 6th International Conference and Field Workshop on Landslides ALPS 90 (Cancelli A, ed). Milano: Ricerca Scientifica ed Educazione Permanente, 79b: 77–88

Jakob M, Weatherly H (2003) A hydroclimatic threshold for landslide initiation on the North Shore Mountains of Vancouver, British Columbia. Geomorphology 54: 137–156

Jan CD, Chen CL (2005) Debris flows caused by Typhoon Herb in Taiwan. In: Debris flow Hazards and Related Phenomena (Jakob M, Hungr O, eds). Springer Berlin Heidelberg, 363–385

Jibson RW (1989) Debris flow in southern Porto Rico. Geological Society of America, Special Paper 236, 29–55

Kanji MA, Massad F, Cruz PT (2003) Debris flows in areas of residual soils: occurrence and characteristics. International Workshop on Occurrence and Mechanisms of Flows in Natural Slopes and Earthfills. Iw-Flows2003, Sorrento: Associacione Geotecnica Italiana 2: 1–11

Keefer DK, Wilson RC, Mark RK, Brabb EE, Brown WM-III, Ellen SD, Harp EL, Wieczorek GF, Alger CS, Zatkin RS (1987) Real-time landslide warning during heavy rainfall. Science 238: 921–925

Kim SK, Hong WP, Kim YM (1991) Prediction of rainfall-triggered landslides in Korea. In: Landslides (Bell DH, ed). Rotterdam: A.A. Balkema, 2: 989–994

Larsen MC, Simon A (1993) A rainfall intensity-duration threshold for landslides in a humid-tropical environment, Puerto Rico. Geogr Ann A 75(1-2): 13–23

Lumb P (1975) Slope failure in Hong Kong. Q J Eng Geol 8:31–65

Marchi L, Arattano M, Deganutti AM (2002) Ten years of debris-flow monitoring in the Moscardo Torrent (Italian Alps). Geomorphology 46: 1–17

Montgomery DR, Dietrich WE (1994) A physically based model for the topographic control of shallow landsliding. Water Resour Res 30(4): 1153–1171

Montgomery DR, Schmidt KM, Greenberg HM (2000) Forest clearing and regional landsliding. Geology 28(4): 311–314

Moser M, Hohensinn F (1983) Geotechnical aspects of soil slips in Alpine regions. Eng Geol 19: 185–211

New M, Hulme M, Jones P (1999) Representing twentieth-century space-time climate variability. Part I: Development of a 1961-90 mean monthly terrestrial climatology. J Climate 12: 829–856

Nilsen TH, Turner BL (1975) Influence of rainfall and ancient landslide deposits on recent landslides (1950-1971) in urban areas of Contra Costa County, California. US Geological Survey Bul 1388

Nilsen TH, Taylor FA, Brabb EE (1976) Recent landslides in Alamanda County, California (1940–71). US Geological Survey Bull 1398

Oberste-lehn D (1976) Slope stability of the Lomerias Muertas area, San Benito County, California. PhD, Stanford University, California

Onodera T, Yoshinaka R, Kazama H (1974) Slope failures caused by heavy rainfall in Japan. In: Proceedings 2nd International Congress of the Int Ass Eng Geol. San Paulo: 11: 1–10

Paronuzzi P, Coccolo A, Garlatti G (1998) Eventi meteorici critici e debris flows nei bacini montani del Friuli. L'Acqua, Sezione I/Memorie: 39–50

Pasuto A, Silvano S (1998). Rainfall as a triggering factor of shallow mass movements. A case study in the Dolomites, Italy. Environ Geol 35(2-3): 184-189

Pedrozzi G (2004) Triggering of landslides in Canton Ticino (Switzerland) and prediction by the rainfall intensità and duration method. Bull Eng Geol Environ 63(4): 281–291

Philip JR (1954) An infiltration equation with physical significance. Soil Sci 77(1): 153–157

Premchitt J, Brand EW, Chen PYM (1994) Rain-induced landslides in Hong Kong, 1972-1992. Asia Engineer, June, 43–51

Reichenbach P, Cardinali M, De Vita P, Guzzetti F (1998) Regional hydrological thresholds for landslides and floods in the Tiber River Basin (Central Italy). Environ Geol 35(2-3): 146–159

Rodolfo KS, Arguden AT (1991) Rain-lahar generation and sediment-delivery systems at Mayon Volcano, Philippines. In: Sedimentation in volcanic settings (Fisher RV, Smith GA, eds). Society of Economic Paleontologists and Mineralogists, Special Publication 45: 71–88

Salvucci GD, Entekabi D (1994) Explicit expressions for Green-Ampt (Delta function diffusivity) infiltration rate and cumulative storage. Water Resour Res 30: 2661–2663

Sandersen F, Bakkehøi S, Hestnes E, Lied K (1996) The influence of meteorological factors on the initiation of debris flows, rockfalls, rockslides and rockmass stability. In: Landslides (Senneset, ed). Rotterdam: A.A. Balkema, 97–114

Sorriso-Valvo M, Agnesi V, Gullà G, Merende L, Antronico L, Di Maggio C, Filice E, Petrucci O, Tansi C (1994) Temporal and spatial occurrence of landsliding and correlation with precipitation time series in Montaldo Uffugo (Calabria) and Imera (Sicilia) areas. In: Temporal Occurrence and Forecasting of Landslides in the European Community (Casale R, Fantechi R, Flageollet JC, eds). Final Report 2: 825–869

Tatizana C, Ogura M, Rocha M, Cerri LES (1987) Analise de correlacao entre chuvas e escorregamentos, Serra do Mar, Municipio de Cubatao. Proceedings 5th Congress Brasiler, Geol Eng San Paolo: 225–236

Terlien MTJ (1998) The determination of statistical and deterministic hydrological landslide-triggering thresholds. Environ Geol 35(2-3): 124–130

Tuñgol NM, Regalado MTM (1996) Rainfall, acoustic flow monitor records, and observed lahars of the Sacobia River in 1992. In: Fire and mud: eruptions and lahars of Mount Pinatubo (Newhall CG, Punongbayan RS, eds). Philippine Institute of Volcanology and Seismology, Quezon City and University of Washington Press, Seattle, 1126 pp

White ID, Mottershead DN, Harrison JJ (1996) Environmental Systems, 2nd Edition. London: Chapman & Hall, 616 pp

Wieczorek GF (1987) Effect of rainfall intensity and duration on debris flows in central Santa Cruz Mountains. In: Debris flow/avalanches: process, recognition, and mitigation (Costa JE, Wieczorek GF, eds). Geological Society of America, Reviews in Engineering Geology, 7: 93–104

Wieczorek GF (1996) Landslide triggering mechanisms. In: Landslides: Investigation and Mitigation (Turner AK, Schuster RL, eds). Washington DC: Transportation Research Board, National Research Council, Special Report, 76–90

Wieczorek GF, Glade T (2005) Climatic factors influencing occurrence of debris flows. In: Debris flow Hazards and Related Phenomena (Jakob M, Hungr O, eds). Springer Berlin Heidelberg, 325–362

Wieczorek GF, Morgan BA, Campbell RH (2000) Debris flow hazards in the Blue Ridge of Central Virginia. Environ Eng Geosci 6: 3–23

Wilson RC (1989) Rainstorms, pore pressures, and debris flows: a theoretical framework. In: Landslides in a semi-arid environment (Morton DM, Sadler PM, eds). California: Publications of the Inland Geological Society, 2: 101–117

Wilson RC (1997) Normalizing rainfall/debris-flow thresholds along the U. S. Pacific coast for long-term variations in precipitation climate. In: Proceedings 1st International Conference on Debris-Flow Hazard Mitigation (Chen CL, ed). San Francisco: American Society of Civil Engineers, 32–43

Wilson RC (2000) Climatic variations in rainfall thresholds for debris-flows activity. In: Proceedings 1st Plinius Conference on Mediterranean Storms (Claps P, Siccardi F, eds). Maratea: 415–424

Wilson RC, Torikai JD, Ellen SD (1992) Development of rainfall thresholds for debris flows in the Honolulu District, Oahu. US Geological Survey Open-File Report 92-521, 45 pp

Wilson RC, Wieczorek GF (1995) Rainfall thresholds for the initiation of debris flow at La Honda, California. Environ Eng Geosci 1(1): 11–27

Wilson RC, Jayko AS (1997) Preliminary Maps Showing Rainfall Thresholds for Debris-Flow Activity, San Francisco Bay Region, California. US Geological Survey Open-File Report 97-745 F

Wu W, Sidle RC (1995) A distributed slope stability model for steep forested basins. Water Resour Res 31: 2097– 2110

Zezere JL, Rodrigues ML (2002) Rainfall thresholds for landsliding in Lisbon Area (Portugal). In: Landslides (Rybar J, Stemberk J, Wagner P, eds). Lisse: A.A. Balkema, 333–338

Zezere JL, Trigo RM, Trigo IF (2005) Shallow and deep landslides induced by rainfall in the Lisbon region (Portugal): assessment of relationships with the North Atlantic Oscillation. Nat Hazard Earth Sys Sci 5: 331–344

Zimmermann M, Mani P, Gamma P, Gsteiger P, Heiniger O, Hunziker G (1997) Murganggefahr und Climaänderung - ein GIS-basierter Ansatz. In: Schlussbericht Nationalen Forschungs Programmes, NFP 31. Zürich: vdf Hochschulverlag AG an der ETH, 161 pp

Table 1. Rainfall and climate variables used in the literature for the definition of rainfall thresholds for the initiation of landslides. Table lists the variable, the units of measure most commonly used for the parameter, and the author(s) who first introduced the parameter. Nomenclature is not consistent in the literature, and different definitions have been used for the same or similar variables.

VARIABLE	*DESCRIPTION*	*UNITS*	*FIRST INTRODUCED*
D	Rainfall duration. The duration of the rainfall event or rainfall period.	h, or days	Caine (1980)
D_C	Duration of the critical rainfall event.	h	Aleotti (2004)
$E_{(h),(d)}$	Cumulative event rainfall. The total rainfall measured from the beginning of the rainfall event to the time of failure. Also known as storm rainfall. "h" indicates the considered period in hours; "d" indicates the considered period in days.	mm	Innes (1983)
E_{MAP}	Normalized cumulative event rainfall. Cumulative event rainfall divided by MAP (E_{MAP}=E/MAP). Also known as normalized storm rainfall.	-	Guidicini and Iwasa (1977)
C	Critical rainfall. The total amount of rainfall from the time of a distinct increase in rainfall intensity (t_0) to the time of the triggering of the first landslide (t_f).	mm	Govi and Sorzana (1980)
C_{MAP}	Normalized critical rainfall. Critical rainfall divided by MAP (C_{MAP}=C/MAP).	-	Govi and Sorzana (1980)
R	Daily rainfall. The total amount of rainfall for the day of the landslide event.	mm	Crozier and Eyles (1980)
R_{MAP}	Normalized daily rainfall. Daily rainfall divided by MAP (R_{MAP}=R/MAP).	mm	Terlien (1998)
I	Rainfall intensity. The amount of precipitation in a period, i.e., the rate of precipitation over the considered period. Depending on the duration of the measuring period, rainfall intensity measures peak or average precipitation rates.	mm/h	Caine (1980)
I_{MAP}	Normalized rainfall intensity. Rainfall intensity divided by MAP (I_{MAP}=I/MAP).	1/h	Cannon (1988)
I_{max}	Maximum hourly rainfall intensity. The maximum hourly rainfall intensity.	mm/h	Onodera et al. (1974)
I_P	Peak rainfall intensity. The highest rainfall intensity (rainfall rate) during a rainfall event. Available from detailed rainfall records.	mm/h	Wilson et al. (1992)
$\hat{I}_{(h)}$	Mean rainfall intensity for final storm period. "h" indicates the considered period, in hours, most commonly from 3 to 24 hours.	mm/h	Govi and Sorzana (1980)
I_C	Critical hourly rainfall intensity.	mm/h	Heyerdahl et al. (2003)
I_f	Rainfall intensity at the time of the slope failure. Available from detailed rainfall records.	mm/h	Aleotti (2004)
I_{fMAP}	Normalized rainfall intensity at the time of the slope failure. Rainfall intensity at the time of the slope failure divided by MAP (I_{fMAP}=I_f/MAP).	1/h	Aleotti (2004)
$A_{(d)}$	Antecedent rainfall. The total (cumulative) precipitation measured before the landslide triggering rainfall event. "d" indicates the considered period in days.	mm	Govi and Sorzana (1980)
A_{MAP}	Normalized antecedent rainfall. Antecedent rainfall divided by MAP (A_{MAP}=A/MAP).	-	Aleotti (2004)
$A_{(y)}$	Antecedent yearly precipitation up to date of the event. The total (cumulative) yearly precipitation measured before the landslide triggering rainfall event.	mm	Guidicini and Iwasa (1977)
$A_{(y)MAP}$	Normalized antecedent yearly precipitation up to date of the event. Antecedent yearly precipitation divided by MAP ($A_{(y)MAP}$=$A_{(y)}$/MAP).	-	Guidicini and Iwasa (1977)
F_C	Sum of normalized antecedent yearly precipitation and normalized event rainfall (F_C=$A_{(y)MAP}$+E_{MAP}). Also known as "final coefficient".	-	Guidicini and Iwasa (1977)
MAP	Mean annual precipitation. For a rain gauge, the long term yearly average precipitation, obtained from historical rainfall records. A proxy for local climatic conditions.	mm	Guidicini and Iwasa (1977)
RDs	Average number of rainy-days in a year. For a rain gauge, the long term yearly average of rainy (or wet) days, obtained from historical rainfall records. A proxy for local climatic conditions.	#	Wilson and Jayko (1997)
RDN	Rainy-day normal. For a rain gauge, the ratio between the MAP and the average number of rainy-days in a year (RDN=MAP/RDs).	mm/#	Wilson and Jayko (1997)
N	Ratio between the MAP of two different (distant) areas.	-	Barbero at al. (2004)

Table 2. Intensity – duration (ID) thresholds for the initiation of landslides. Extent: G, global threshold; R, regional threshold; L, local threshold. Area, the area where the threshold was defined. Landslide type: A, all types; D, debris flow; S, soil slip; Sh, shallow landslide, L, lahar. Rainfall intensity in mm/hr, rainfall duration in hours. Dots indicate thresholds defined inside the CADSES area. Equations in italics were estimated. Source: 1, Caine (1980); 2, Moser and Hohensinn (1983); 3, Cancelli and Nova (1985); 4-5, Cannon and Ellen (1985); 6, Wieczorek (1987); 7-15, Jibson (1989); 16, Guadagno (1991); 17, Rodolfo and Arguden (1991); 18, Ceriani et al. (1992); 19, Larsen and Simon (1993); 20, Arboleda and Martinez (1996); 21, Clarizia et al. (1996); 22, Tuñgol and Regalado (1996); 23, Zimmermann et al. (1997); 24, Paronuzzi et al. (1998); 25-30, Bolley and Olliaro (1999); 31, Calcaterra et al. (2000); 32, Montgomery et al. (2000); 33, Wieczorek et al. (2000); 34, Crosta and Frattini (2001); 35, Marchi et al. (2002); 36, Ahmad (2003); 37, Jakob and Weatherly (2003); 38, Aleotti (2004); 39, Barbero et al. (2004); 40, Floris et al. (2004); 41, Baum (2005); 42, Cannon and Gartner (2005); 43, Chien-Yuan et al. (2005); 44, Corominas et al. (2005); 45-48, Giannecchini (2005); 49, Hong et al. (2005); 50-51, Jan and Chen (2005); 52, Zezere et al. (2005). See also Figure 2.

#	EXTENT	AREA	LANDSLIDE TYPE	EQUATION	RANGE	NOTES
1	G	World	Sh, D	$I = 14.82 \times D^{-0.39}$	$0.167 < D < 500$	
2	R	Carinthia and E Tyrol, Austria	S	$I = 41.66 \times D^{-0.77}$	$1 < D < 1000$	●
3	L	Valtellina, Lombardy, N Italy	S	$I = 44.668 \times D^{-0.78}$	$1 < D < 1000$	●
4	L	San Francisco Bay Region, California	D	$I = 6.9+38 \times D^{-1.00}$	$2 < D < 24$	High MAP
5	L	San Francisco Bay Region, California	D	$I = 2.5+300 \times D^{-2.0}$	$5.5 < D < 24$	Low MAP
6	L	Central Santa Cruz Mountains, California	D	$I = 1.7+9 \times D^{-1.00}$	$1 < D < 6.5$	
7	R	Indonesia	D	$I = 92.06-10.68 \times D^{1.0}$	$2 < D < 4$	
8	R	Puerto Rico	D	$I = 66.18 \times D^{-0.52}$	$0.5 < D < 12$	
9	R	Brazil	D	$I = 63.38-22.19 \times D^{1.0}$	$0.5 < D < 2$	
10	R	China	D	$I = 49.11-6.81 \times D^{1.0}$	$1 < D < 5$	
11	L	Hong Kong	D	$I = 41.83 \times D^{-0.58}$	$1 < D < 12$	
12	R	Japan	D	$I = 39.71 \times D^{-0.62}$	$0.5 < D < 12$	
13	R	California	D	$I = 35.23 \times D^{-0.54}$	$3 < D < 12$	
14	R	California	D	$I = 26.51 \times D^{-0.19}$	$0.5 < D < 12$	
15	G	World	D	$I = 30.53 \times D^{-0.57}$	$0.5 < D < 12$	Lower envelope
16	R	Peri-Vesuvian area, Campania Region, S Italy	D	$I = 176.40 \times D^{-0.90}$	$0.1 < D < 1000$	Volcanic soils
17	L	Mayon, Philippine	L	$I = 27.3 \times D^{-0.38}$	$0.167 < D < 3$	
18	R	Lombardy, N Italy	A	$I = 20.1 \times D^{-0.55}$	$1 < D < 1000$	●
19	R	Puerto Rico	A	$I = 91.46 \times D^{-0.82}$	$2 < D < 312$	
20	L	Pasig-Potrero River, Philippine	L	$I = 9.23 \times D^{-0.37}$	$0.08 < D < 7.92$	
21	G	World	S	$I = 10 \times D^{-0.77}$	$0.1 < D < 1000$	
22	L	Sacobia River, Philippine	L	$I = 5.94 \times D^{-1.50}$	$0.167 < D < 3$	
23	R	Switzerland	A	$I = 32 \times D^{-0.70}$	$1 < D < 45$	
24	R	NE Alps, Italy	D	$I = 47.742 \times D^{-0.507}$	$0.1 < D < 24$	●
25	L	Rho Basin, Susa Valley, Piedmont, NW Italy	D	$I = 9.521 \times D^{-0.4955}$	$1 < D < 24$	A > 14% of MAP
26	L	Rho Basin, Susa Valley, Piedmont, NW Italy	D	$I = 11.698 \times D^{-0.4783}$	$1 < D < 24$	A < 14% of MAP
27	L	Perilleux Basin, Piedmont, NW Italy	D	$I = 11.00 \times D^{-0.4459}$	$1 < D < 24$	A > 9% of MAP
28	L	Perilleux Basin, Piedmont, NW Italy	D	$I = 10.67 \times D^{-0.5043}$	$1 < D < 24$	A < 9% of MAP
29	L	Champeyron Basin, Piedmont, NW Italy	D	$I = 12.649 \times D^{-0.5324}$	$1 < D < 24$	A > 14% of MAP
30	L	Champeyron Basin, Piedmont, NW Italy	D	$I = 18.675 \times D^{-0.565}$	$1 < D < 24$	A < 14% of MAP
31	R	Campania, S Italy	A	$I = 28.10 \times D^{-0.74}$	$1 < D < 600$	
32	L	Mettman Ridge, Oregon	A	$I = 9.9 \times D^{-0.52}$	$1 < D < 170$	
33	L	Blue Ridge, Madison County, Virginia	D	$I = 116.48 \times D^{-0.63}$	$2 < D < 16$	
34	G	World	Sh	$I = 0.48+7.2 \times D^{-1.00}$	$0.1 < D < 1000$	
35	L	Moscardo Torrent, NE Italy	A	$I = 15 \times D^{-0.70}$	$1 < D < 30$	●
36	R	Eastern Jamaica	Sh	$I = 11.5 \times D^{-0.26}$	$1 < D < 150$	
37	R	North Shore Mountains, Vancouver, Canada	Sh	$I = 4.0 \times D^{-0.45}$	$0.1 < D < 150$	
38	R	Piedmont, NW Italy	Sh	$I = 19 \times D^{-0.50}$	$4 < D < 150$	
39	L	Piedmont, NW Italy	A	$I = 44.668 \times D^{-0.78} \times N$	$1 < D < 1000$	N = ratio of MAPs
40	L	Valzangona, N Apennines, Italy	A	$I = 18.83 \times D^{-0.59}$	$24 < D < 3360$	●
41	L	Seattle Area, Washington	S	$I = 82.73 \times D^{-1.13}$	$20 < D < 55$	
42	G	World	D	$I = 7.00 \times D^{-0.60}$	$0.1 < D < 3$	For burnt areas
43	R	Taiwan	A	$I = 115.47 \times D^{-0.80}$	$1 < D < 400$	

#	EXTENT	AREA	LANDSLIDE TYPE	EQUATION	RANGE	NOTES
44	R	Pyrenees, Spain	A	$I = 17.96 \times D^{-0.59}$	D > 168	For low Permeability clay
45	L	Apuane Alps, Tuscany, Italy	Sh	$I = 26.871 \times D^{-0.638}$	0.1 < D < 35	Lower threshold
46	L	Apuane Alps, Tuscany, Italy	Sh	$I = 85.584 \times D^{-0.781}$	0.1 < D < 35	Upper threshold
47	L	Apuane Alps, Tuscany, Italy	Sh	$I = 38.363 \times D^{-0.743}$	0.1 < D ≤ 12	Lower threshold
48	L	Apuane Alps, Tuscany, Italy	Sh	$I = 76.199 \times D^{-0.692}$	0.1 < D ≤ 12	Upper threshold
49	R	Shikoku Island, Japan	A	$I = 1.35+55 \times D^{-1.0}$	24 < D < 300	
50	R	Central Taiwan	D	$I = 13.5 \times D^{-0.20}$	0.7 < D < 40	Before Chi-Chi earthquake
51	R	Central Taiwan	D	$I = 6.7 \times D^{-0.20}$	0.7 < D < 40	After Chi-Chi earthquake
52	L	N of Lisbon, Portugal	A	$I = 84.3 \times D^{-0.57}$	0.1 < D < 2000	

Table 3. Normalized intensity – duration (Normalized ID) thresholds for the initiation of landslides. Extent: G, global threshold; R, regional threshold; L, local threshold. Area, the area where the threshold was defined. Landslide type: D, debris flow; Sh, shallow landslide. Normalized rainfall intensity in h^{-1}, rainfall duration in hours. Equations in italics were estimated. Dots indicate thresholds defined inside the CADSES area. Source: 53, Cannon (1988); 54-61, Jibson (1989); 62, Ceriani et al. (1992); 63, Paronuzzi et al. (1998); 64, Wieczorek et al. (2000); 65-68, Aleotti et al. (2002); 69, Bacchini and Zannoni (2003); 70-71, Aleotti (2004). See also Figure 3.

#	EXTENT	AREA	LANDSLIDE TYPE	EQUATION	RANGE	NOTES
53	L	San Francisco Bay Region, California	D	$D = 46.1\text{-}3.6\cdot10^{3}\times I_{MAP} + 7.4\cdot10^{4}\times(I_{MAP})^{2}$	$1 < D < 24$	
54	R	Indonesia	D	$I_{MAP} = 0.07\text{-}0.01\times D^{1}$	$2 < D < 4$	
55	R	Puerto Rico	D	$I_{MAP} = 0.06\times D^{-0.59}$	$1 < D < 12$	
56	R	Brazil	D	$I_{MAP} = 0.06\text{-}0.02\times D^{1}$	$0.5 < D < 2$	
57	L	Hong Kong	D	$I_{MAP} = 0.02\times D^{-0.68}$	$1 < D < 12$	
58	R	Japan	D	$I_{MAP} = 0.03\times D^{-0.63}$	$1 < D < 12$	
59	R	California	D	$I_{MAP} = 0.03\times D^{-0.33}$	$1 < D < 12$	
60	R	California	D	$I_{MAP} = 0.03\times D^{-0.21}$	$0.5 < D < 8$	
61	G	World	D	$I_{MAP} = 0.02\times D^{-0.65}$	$0.5 < D < 12$	Lower envelope
62	R	Central Alps, Lombardy, N Italy	D	$I_{MAP} = 2.0\times D^{-0.55}$	$1 < D < 100$	●
63	R	NE Alps, Italy	D	$I_{MAP} = 0.026\times D^{-0.507}$	$0.1 < D < 24$	●
64	L	Blue Ridge, Madison County, Virginia	D	$I_{MAP} = 0.09\times D^{-0.63}$	$2 < D < 16$	
65	L	Val Sesia, Piedmont, NW Italy	Sh	$I_{MAP} = 1.1122\times D^{-0.2476}$	$1 < D < 200$	
66	L	Val d'Ossola, Piedmont, NW Italy	Sh	$I_{MAP} = 0.6222\times D^{-0.2282}$	$1 < D < 200$	
67	L	Valli di Lanzo, Piedmont, NW Italy	Sh	$I_{MAP} = 1.6058\times D^{-0.4644}$	$1 < D < 200$	
68	L	Val d'Orco, Piedmont, NW Italy	Sh	$I_{MAP} = 1.6832\times D^{-0.5533}$	$1 < D < 200$	
69	L	Cancia, Dolomites, NE Italy	D	$I_{MAP} = 0.74\times D^{-0.56}$	$0.1 < D < 100$	●
70	R	Piedmont, NW Italy	Sh	$I_{MAP} = 0.76\times D^{-0.33}$	$2 < D < 150$	
71	R	Piedmont, NW Italy	Sh	$I_{fMAP} = 4.62\times D^{-0.79}$	$2 < D < 150$	

Table 4. Rainfall thresholds for the initiation of landslides based on measurements of the event precipitation. Extent: R, regional threshold; L, local threshold. Area, the area where the threshold was defined. Landslide type: A, all types; D, debris flow; S, soil slip; Sh, shallow landslide. Dot indicates threshold defined inside the CADSES area. Source: 72, Endo (1970); 73, Campbell (1975); 74, Lumb (1975); 75, Nilsen and Turner (1975); 76, Nilsen et al. (1976); 77, Oberste-lehn (1976); 78, Guidicini and Iwasa (1977); 79, Govi and Sorzana (1980); 80, Mark and Newman, cited in Cannon and Ellen (1985); 81, Canuti et al. (1985); 82-83, Bhandari et al. (1991); 84, Sorriso-Valvo et al. (1994); 85, Corominas and Moya (1996); 86, Pasuto and Silvano (1998); 87, Corominas and Moya (1999); 88, Biafiore et al. (2002); 89, Bell and Maud (2000).

#	Extent	Area	Landslide Type	Threshold	Notes
72	L	Hokkaido area, Japan	A	$R > 200$ mm	
73	R	Los Angeles area, California, USA	A	$R > 235$ mm	
74	L	Hong Kong	S	$A_{15d} > 50$ mm and $R > 50$ mm $A_{15d} > 200$ mm and $R > 100$ mm $A_{15d} > 350$ mm and $R > 100$ mm	Minor events Severe events Very severe events
75	R	Contra Costa County, California, USA	Sh	$E > 177.8$ mm	Abundant landslides
76	R	Alamanda County, California, USA	A	$R > 180$ mm	
77	R	San Benito County, California, USA	A	$E > 250$ mm	
78	R	Brazil	A	$E_{MAP} > 0.12$ $0.08 < E_{MAP} < 0.12$ $E_{MAP} < 0.08$	Independently of antecedent rainfall Depending on antecedent rainfall Not likely to trigger landslides
79	R	Piedmont Region, NW Italy	A	$0.10 < E_{MAP} < 0.25$ $0.22 < E_{MAP} < 0.31$ $0.28 < E_{MAP} < 0.38$	3 to 15 landslides per km^2 up to 30 landslides per km^2 up to 60 landslides per km^2
80	R	San Francisco Bay region, California, USA	Sh	$E > 254$ mm	Greater propensity for landslides
81	R	Italy	A	$E_{1\text{-}3d} > 100$ mm	For marly, arenaceous rocks
82	R	Sri Lanka	A	$E_{3d} > 200$ mm	
83	R	Eastern Himalaya	A	$E_{MAP} < 0.05$ $0.05 < E_{MAP} < 0.10$ $0.10 < E_{MAP} < 0.20$ $E_{MAP} > 0.20$	Low probability of landslides Intermediate probability of landslides High probability of landslides Landslides will always occur
84	L	Montaldo area, Calabria, Italy	A	$A_{50d} > 530$ mm	
85	L	Llobregat valley, E Pyrenees, Spain	Sh, D	$R > 160 – 200$ mm	Without antecedent rainfall
86	L	Cordevole River Basin, Belluno, Veneto	Sh	$A_{15d} > 250$ mm and $R > 70$ mm	•
87	R	E Pyrenees, Spain	A	$E > 180$-190 mm in 24-36 h $E > 300$ mm in 24-48 h	Slight shallow landsliding Widespread landsliding
88	L	Sarno, Campania Region, S Italy	A	$R > 55$ mm $R > 75$ mm	For saturated pyroclastic soils, lower threshold For saturated pyroclastic soils, upper threshold
89	L	Natal Group, Durban area, KwaZulu-Natal, South Africa	A	$A_{15d} > 450$ mm $E > 100$-150 mm in 2 hours $E_{MAP} < 0.12$ $0.12 < E_{MAP} < 0.16$ $0.16 < E_{MAP} < 0.20$ $E_{MAP} > 0.20$	 Landslides do not occur Minor events (1 or 2 landslides) Moderate events (3 to 6 landslides) Severe events (> 10 landslides)

Table 5. Rainfall event – duration (ED) thresholds and normalized rainfall event – duration thresholds for the initiation of landslides. Extent: G, global threshold; R, regional threshold, L, local threshold. Area, the area where the threshold was defined. Landslide type: A, all types; D, debris flow; Sh, shallow landslide. Cumulative event rainfall in mm, rainfall duration in hours. Source: 90, Caine (1980); 91, Innes (1983); 92-95, Wilson et al. (1992); 96, Sandersen et al. (1996); 97, Corominas and Moya (1999); 98-99, Annunziati et al. (2000); 100, Zezere and Rodrigues (2002); 101, Kanji et al. (2003); 102, Aleotti (2004); 103-104, Giannecchini (2005). See also Figure 4.

#	Extent	Area	Landslide Type	equation	Range	Notes
90	G	World	Sh, D	$E = 14.82 \times D^{0.61}$	$0.167 < D < 500$	
91	G	World	D	$E = 4.93 \times D^{0.504}$	$0.1 < D < 100$	
92	L	Nuuanu, Honolulu, Hawaii	D	$E = 13.08+2.16\times D$ $E = 9.91+3.22\times D$	$1 \le D \le 3$ $3 < D \le 6$	Safety (minimum) threshold
93	L	Nuuanu, Honolulu, Hawaii	D	$E = 12.45+27.18\times D$ $E = 48.26+15.24\times D$	$1 \le D \le 3$ $3 < D \le 6$	For abundant landslides
94	L	Kaluanui, Honolulu, Hawaii	D	$E = 13.84+12.83\times D$ $E = 15.75+12.19\times D$	$1 \le D \le 3$ $3 < D \le 6$	Safety (minimum) threshold
95	L	Kaluanui, Honolulu, Hawaii	D	$E = 8.76+32.64\times D$ $E = 53.34+17.78\times D$	$1 \le D \le 3$ $3 < D \le 6$	For abundant landslides
96	R	Norway	D	$C_{MAP} = 1.2\times D^{0.6}$	$0.1 < D < 180$	
97	L	Llobregat River basin, E Pyrenees, Spain	A	$E = 133+0.19\times D$	$84 < D < 1092$	
98	L	Apuan Alps, Tuscany, Italy	D	$E = 27.50 + 22.50\times D$ $E = 66.67 + 9.44\times D$ $E = 165.00 + 1.25\times D$	$1 \le D \le 3$ $3 < D \le 12$ $12 < D \le 24$	Minimum threshold
99	L	Apuan Alps, Tuscany, Italy	D	$E = 45.00 + 55.00\times D$ $E = 150.00 + 20.00\times D$ $E = 375.00 + 1.25\times D$	$1 \le D \le 3$ $3 < D \le 12$ $12 < D \le 24$	For catastrophic landslides
100	L	N of Lisbon, Portugal	A	$E = 70+0.2625\times D$	$0.1 < D < 2400$	
101	R	Brazil	D	$E = 22.4\times D^{0.41}$	$1 < D < 10{,}000$	
102	R	Piedmont, NW Italy	Sh	$C_{MAP} = -10.465 + 8.35\times \ln D$	$5 < D < 30$	
103	L	Apuan Alps, Tuscany, Italy	Sh	$E_{MAP} = 1.0711+0.1974\times D$	$1 < D < 30$	Lower threshold
104	L	Apuan Alps, Tuscany, Italy	Sh	$E_{MAP} = 5.1198+0.2032\times D$	$1 < D < 30$	Upper threshold

Table 6. Rainfall event – intensity (EI) thresholds and normalized rainfall event – intensity thresholds for the initiation of landslides. Extent: G, global threshold; R, regional threshold; L, local threshold. Area, the area where the threshold was defined. Landslide type: A, all types; D, debris flow; S, Soil slide; Sl, slide; E, earth flow; M, mud flow; Sh, shallow landslide; L, lahar. Dot indicates a threshold defined inside the CADSES area. Source: 105-107, Onodera et al. (1974); 108, Govi et al. (1985); 109, Tatizana et al. (1987); 110-116, Jibson (1989); 117, Bacchini and Zannoni (2003); 118, Heyerdahl et al. (2003); 119-121, Aleotti et al. (2002); 122-123, Giannecchini (2005); 124, Hong et al. (2005).

#	EXTENT	AREA	LANDSLIDE TYPE	EQUATION	RANGE	NOTES
105	R	Chiba and Kanagawa prefectures, central Japan	Sh	$I_{max} = 390 \times E^{-0.38}$	$0 < E < 400$	Upper threshold (major disaster)
106	R	Chiba and Kanagawa prefectures, central Japan	Sh	$I_{max} = 290 \times E^{-0.38}$	$0 < E < 300$	Intermediate threshold
107	R	Chiba and Kanagawa prefectures, central Japan	Sh	$I_{max} = 150 \times E^{-0.38}$	$0 < E < 200$	Lower threshold
108	R	Piedmont, NW Italy	S, D, M	$E_{MAP} = 0.13 \times I^{0.12}$	$1.5 \le I \le 8$	For winter and spring
				$E_{MAP} = 0.30 \times I^{0.39}$	$3.5 \le I \le 20$	For summer and autumn
				$E_{MAP} = 0.72 \times I^{0.68}$	$20 \le I \le 50$	For summer
109	R	Serra do Mar, Cubatao, Brazil	Sl, E	$I = 2603 \times E_{96h}^{-0.933}$	$0 < E_{96h} < 500$	Human induced failures
110	R	Japan	D	$I = 112.25 - 0.20 \times E$	$165 < E < 440$	
111	R	Japan	D	$I = 67.38 \times e^{-0.0023 \times E}$	$50 < E < 400$	
112	R	California	D	$I = 31.99 - 0.10 \times E$	$0 < E < 315$	
113	R	Japan	D	$I_{MAP} = 0.04 - 0.19 \times E_{MAP}$	$0 < E_{MAP} < 0.22$	
114	R	Japan	D	$I_{MAP} = 0.04 \times e^{-3.55 \times E_{MAP}}$	$0.03 < E_{MAP} < 0.25$	
115	R	Brazil	D	$I_{MAP} = 0.004 \times E_{MAP}^{-0.92}$	$0.04 < E_{MAP} < 0.4$	
116	G	World	D	$I_{MAP} = 0.003 \times E_{MAP}^{-0.74}$	$0.03 < E_{MAP} < 0.4$	Lower envelope
117	L	Cancia, NE Italy	D	$E_{MAP} = 3.93\text{-}1.36 \times \ln I$	$I > 2$	•
118	R	Nicaragua and El Salvador	L	$I_C = 258 \times E_{96h}^{-0.32}$	$0 < E_{96h} < 500$	
119	R	Piedmont, NW Italy	Sh	$I_{MAP}=0.54\text{-}0.09 \times \ln C_{MAP}$	$7 < C_{MAP} < 60$	General threshold
120	R	Piedmont, NW Italy	Sh	$I_{MAP}=0.51\text{-}0.09 \times \ln C_{MAP}$	$7 < C_{MAP} < 60$	Low magnitude
121	R	Piedmont, NW Italy	Sh	$I_{MAP}=0.70\text{-}0.09 \times \ln C_{MAP}$	$7 < C_{MAP} < 60$	High magnitude
122	L	Apuane Alps, Tuscany, Italy	Sh	$E_{MAP} = 6.5471 - 1.4916 \times \ln I$	$3 < I < 50$	Lower threshold
123	L	Apuane Alps, Tuscany, Italy	Sh	$E_{MAP} = 14.183 - 2.4812 \times \ln I$	$10 < I < 50$	Upper threshold
124	R	Shikoku Island, Japan	A	$I = 1000 \times E^{-1.23}$	$100 < E < 230$	

FIGURE CAPTIONS

Figure 1. Location of the study area in Europe. The CADSES area, shown in grey, extends for more than 2.7×10^6 km^2 and comprises regions belonging to 18 European countries. Circles show approximate location of sites or areas for which rainfall characteristics resulting in landslides were available. Dots show approximate location of sites or regions for which rainfall thresholds for the initiation of landslides have been determined.

Figure 2. Rainfall intensity-duration (ID) thresholds. Numbers refer to # in Table 2. Legend: very thick line, global threshold; thick line, regional threshold; thin line, local threshold. Black lines show global thresholds and thresholds determined for regions or areas pertaining to the CADSES area. Grey lines show thresholds determined for regions or areas not-pertaining to the CADSES area.

Figure 3. Normalized rainfall intensity-duration (ID) thresholds. Numbers refer to # in Table 3. Legend: very thick line, global threshold; thick line, regional threshold; thin line, local threshold. Black lines show global thresholds and thresholds determined for regions or areas pertaining to the CADSES area. Grey lines show thresholds determined for regions or areas not-pertaining to the CADSES area.

Figure 4. Rainfall event – rainfall duration (ED) thresholds. Numbers refer to # in Table 5. Legend: very thick line, global threshold; thick line, regional threshold; thin line, local threshold. Black lines show global thresholds applicable to the CADSES area.

Figure 5. Statistics obtained from the database of rainfall events that resulted and did not result in landslides in the CADSES area and the neighbouring regions (see Figure 1). (A) Geographical precision for the location of the rainfall and landslide event. (B) Proportion of rainfall events that resulted or did not result in landslides. (C) Landslide events for which antecedent rainfall information is available. (D) Landslide types, passed chiefly on estimated landslide depth. (E) Number of reported landslides for each rainfall event. (F) Information on the exact or approximate time, date or period of failure. (G) Information on lithology. (H) Climate classification, based on the Köppen climate classification system; H - Highland and mountain

climate, ET – Polar tundra, Dfc – Severe mid-latitude subartic, Dfb – Severe mid-latitude humid continental, Csa – Mild mid-latitude Mediterranean, Cfb – Mild mid-latitude marine west coast. (I) Frequency of rainfall events for classes of MAP. (J) Frequency of rainfall events for classes of the average number of rainy-days (RDs).

Figure 6. Rainfall intensity-duration (ID) thresholds for the initiation of landslides in the CADSES area. (A) ID data; filled symbols, rainfall conditions that resulted in landslides; open circles, rainfall conditions that did not result in landslides. Shape of symbol indicates landslide type; square = debris flow, diamond = soil slip, dot = shallow landslide, triangle = unknown type. Size of symbol indicates number of the reported landslides; small symbol = single event, large symbol = multiple events. (B) Percentiles plot; lines show, from bottom to top, 2nd, 5th, 10th, 20th, 30th, 40th, 50th, 60th, 70th, 80th and 90th percentiles. (C) Rainfall ID thresholds. Grey line shows threshold from raw ID data (filled symbols in (A)). Black lines show thresholds obtained from 2nd percentile estimates (dots in (B)), for two different rainfall periods. Filled dots show rainfall conditions that resulted in landslides; open circles show rainfall conditions that did not result in landslides.

Figure 7. Validation of obtained ID and normalized-ID thresholds. For rainfall events that resulted in landslides, grey portion of vertical bar shows percentage of events located above the established threshold, and black portion of vertical bar shows percentage of events below the threshold (false negatives). (A), (B), (C) show validation of ID thresholds. (D), (E), (F) show validation of $I_{MAP}D$ thresholds. (G), (H) and (I) show validation of $I_{RDN}D$ thresholds. (A), (D) (G), all data. (B), (E), (H), subsets of events for mild mid-latitude climates. (C), (F), (I), subsets of events for highland, polar, sub-artic, and severe mid-latitude climates.

Figure 8. Rainfall ID thresholds for the initiation of landslides in the CADSES area, for different climate regimes. Left plots, mild, mid-latitude climates; right, highlands, severe mid-latitude, polar and sub-artic climates. (A), (B), ID data; filled symbols, rainfall conditions that resulted in landslides; open circles, rainfall conditions that did not result in landslides. Shape of symbol indicates landslide type; square = debris flow, diamond = soil slip, dot = shallow landslide, triangle = unknown type. Size of symbol indicates number of the reported landslides; small symbol = single event, large symbol = multiple events. (C), (D), percentiles plot; lines show, from bottom to

top, 2nd, 5th, 10th, 20th, 30th, 40th, 50th, 60th, 70th, 80th and 90th percentiles. (E), (F), rainfall ID thresholds. Grey line shows threshold from raw ID data (filled symbols in (A) and (B)); black lines show thresholds obtained from 2nd percentile estimates (dots in (C) and (D)), for different rainfall periods. Filled dots show rainfall conditions that resulted in landslides; open circles show rainfall conditions that did not result in landslides.

Figure 9. Normalized ID thresholds for the initiation of landslides in the CADSES area. Left plots, I_{MAP}-D thresholds; right, I_{RDN}-D thresholds. Plots in the upper raw show thresholds for all normalized ID data. Plots in the central raw show thresholds for subsets of events in mild mid-latitude climates. Plots in the lower raw show thresholds for subsets of events for highland, polar, sub-artic, and severe mid-latitude climates. Grey line shows threshold from raw ID data. Black lines show thresholds obtained from 2nd percentile estimates, for different rainfall periods. Filled dots show rainfall conditions that resulted in landslides; open circles show rainfall conditions that did not result in landslides.

Figure 10. Comparison between the ID thresholds defined in this study, global (worldwide) ID thresholds, local and regional thresholds defined for the CADSES area available in the literature, and thresholds defined for the Piedmont Region. 1, Caine (1980); 2, Innes (1983); 3, Jibson (1989); 4, Clarizia et al. (1996); 5, Crosta and Frattini (2001); 6, Moser and Hohensinn (1983); 7, Cancelli and Nova (1985); 8, Ceriani et al. (1992); 9, Paronuzzi et al. (1998); 10, Marchi et al. (2002); 11, Floris et al. (2004); 12-17, Bolley and Olliaro (1999); 18, Aleotti (2004). Grey lines show thresholds defined in this work from the entire ensemble of ID data (Figure 6C), from 2nd percentile estimates for entire ensemble of ID data, for short and long rainfall periods (Figure 6C).

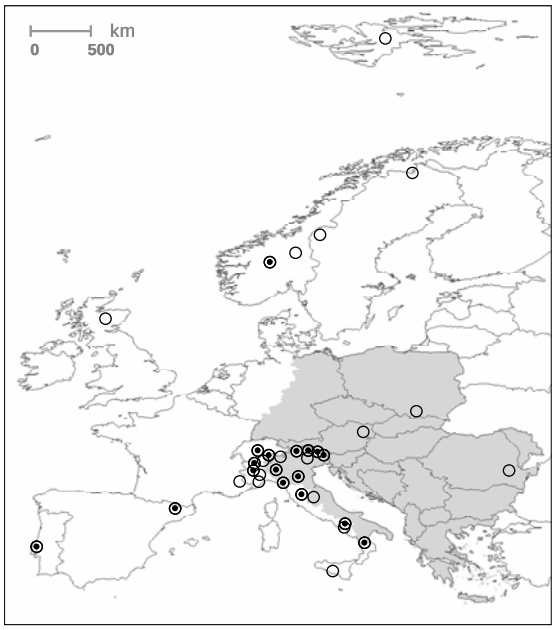

Figure 1

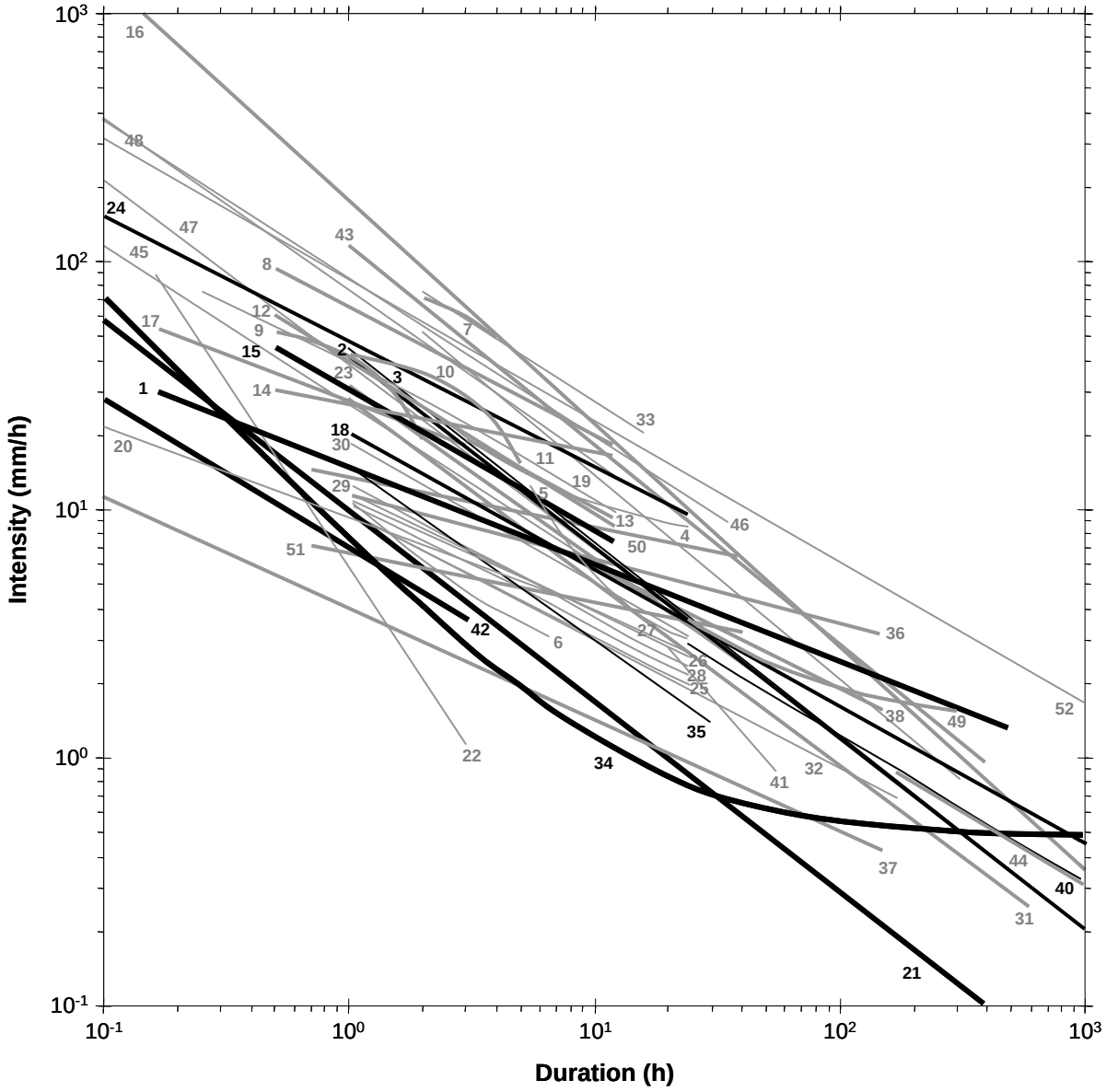
Intensity (mm/h)
Duration (h)
10³
10²
10¹
10⁰
10⁻¹
10⁻¹
10⁰
10¹
10²
10³
16
48
24
47
43
45
8
12
9
7
17
15
2
23
10
3
14
1
33
18
30
20
11
19
29
5
13
46
4
50
51
36
42
6
27
26
28
25
52
38
49
35
22
34
32
41
37
44
40
31
21

Figure 2

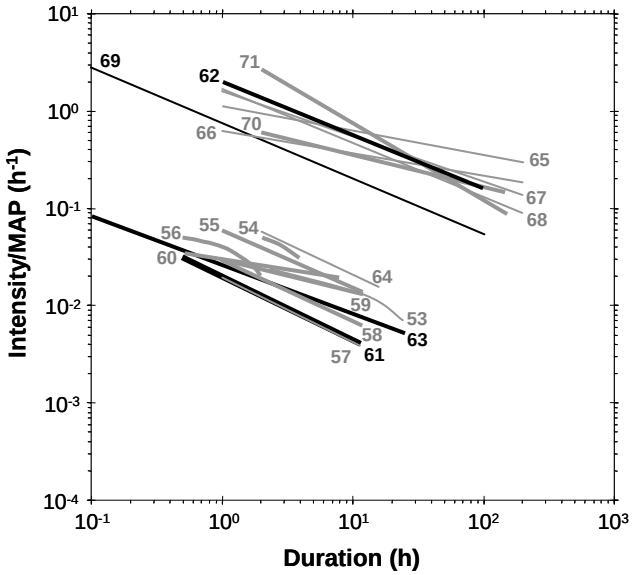
Intensity/MAP (h-1)
Duration (h)
69
62
71
66
70
65
67
68
56
55
54
60
64
59
53
58
63
57
61

Figure 3

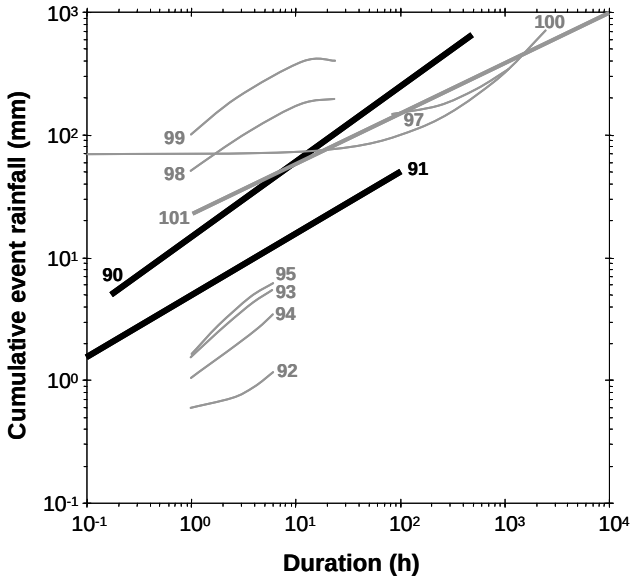
Cumulative event rainfall (mm)
Duration (h)
10³
10²
10¹
10⁰
10⁻¹
10⁻¹
10⁰
10¹
10²
10³
10⁴
99
98
101
97
100
90
91
95
93
94
92

Figure 4

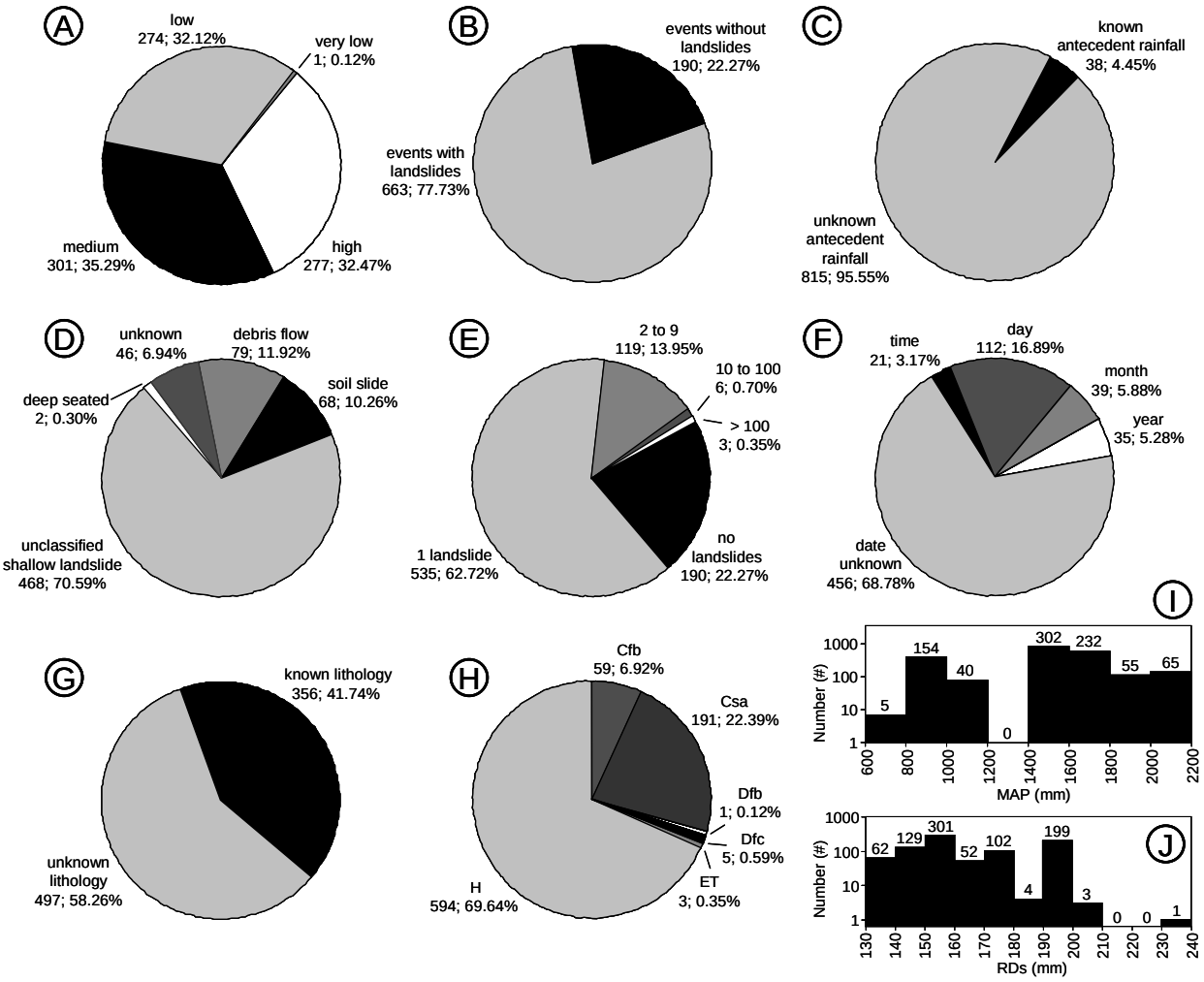
A
low
274; 32.12%
very low
1; 0.12%
medium
301; 35.29%
high
277; 32.47%
B
events without
landslides
190; 22.27%
events with
landslides
663; 77.73%
C
known
antecedent rainfall
38; 4.45%
unknown
antecedent
rainfall
815; 95.55%
D
unknown
46; 6.94%
debris flow
79; 11.92%
soil slide
68; 10.26%
deep seated
2; 0.30%
unclassified
shallow landslide
468; 70.59%
E
2 to 9
119; 13.95%
10 to 100
6; 0.70%
> 100
3; 0.35%
1 landslide
535; 62.72%
no
landslides
190; 22.27%
F
time
21; 3.17%
day
112; 16.89%
month
39; 5.88%
year
35; 5.28%
date
unknown
456; 68.78%
G
known lithology
356; 41.74%
unknown
lithology
497; 58.26%
H
Cfb
59; 6.92%
Csa
191; 22.39%
Dfb
1; 0.12%
Dfc
5; 0.59%
ET
3; 0.35%
H
594; 69.64%
I
Number (#)
1000
100
10
1
5
154
40
0
302
232
55
65
600
800
1000
1200
1400
1600
1800
2000
2200
MAP (mm)
J
Number (#)
1000
100
10
1
62
129
301
52
102
4
199
3
0
0
1
130
140
150
160
170
180
190
200
210
220
230
240
RDs (mm)

Figure 5

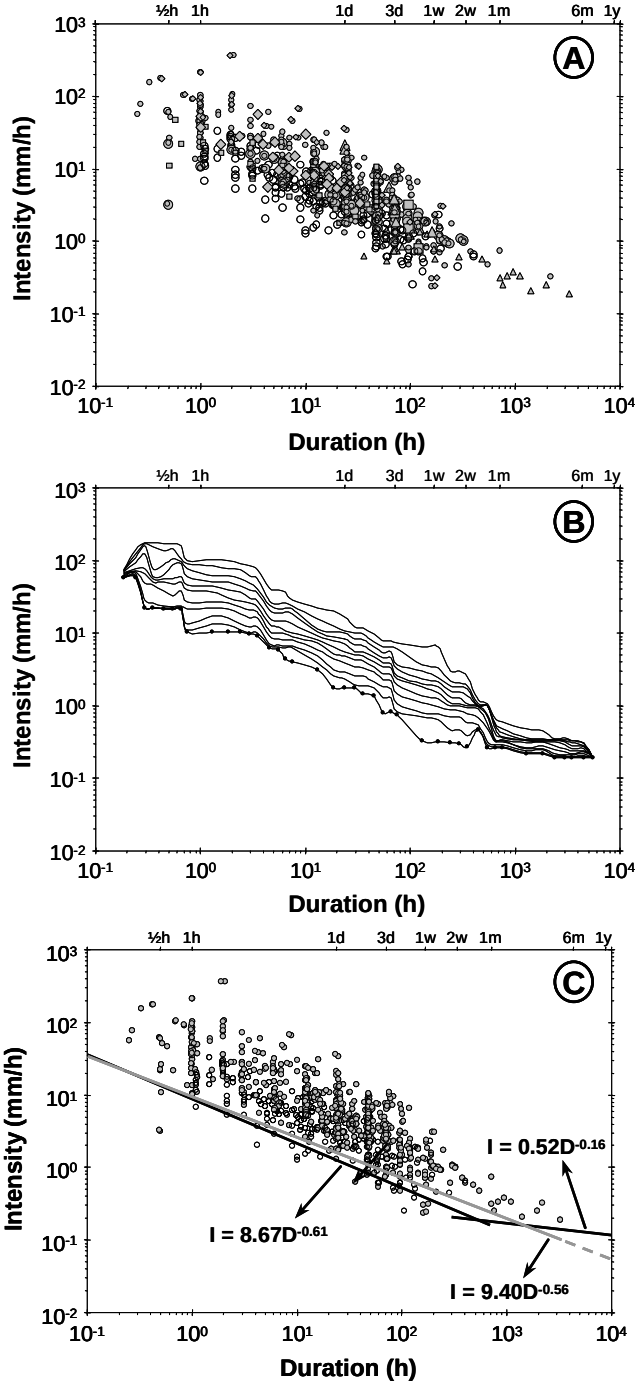
½h 1h 1d 3d 1w 2w 1m 6m 1y
A
Intensity (mm/h)
Duration (h)
B
C
I = 0.52D-0.16
I = 8.67D-0.61
I = 9.40D-0.56

Figure 6

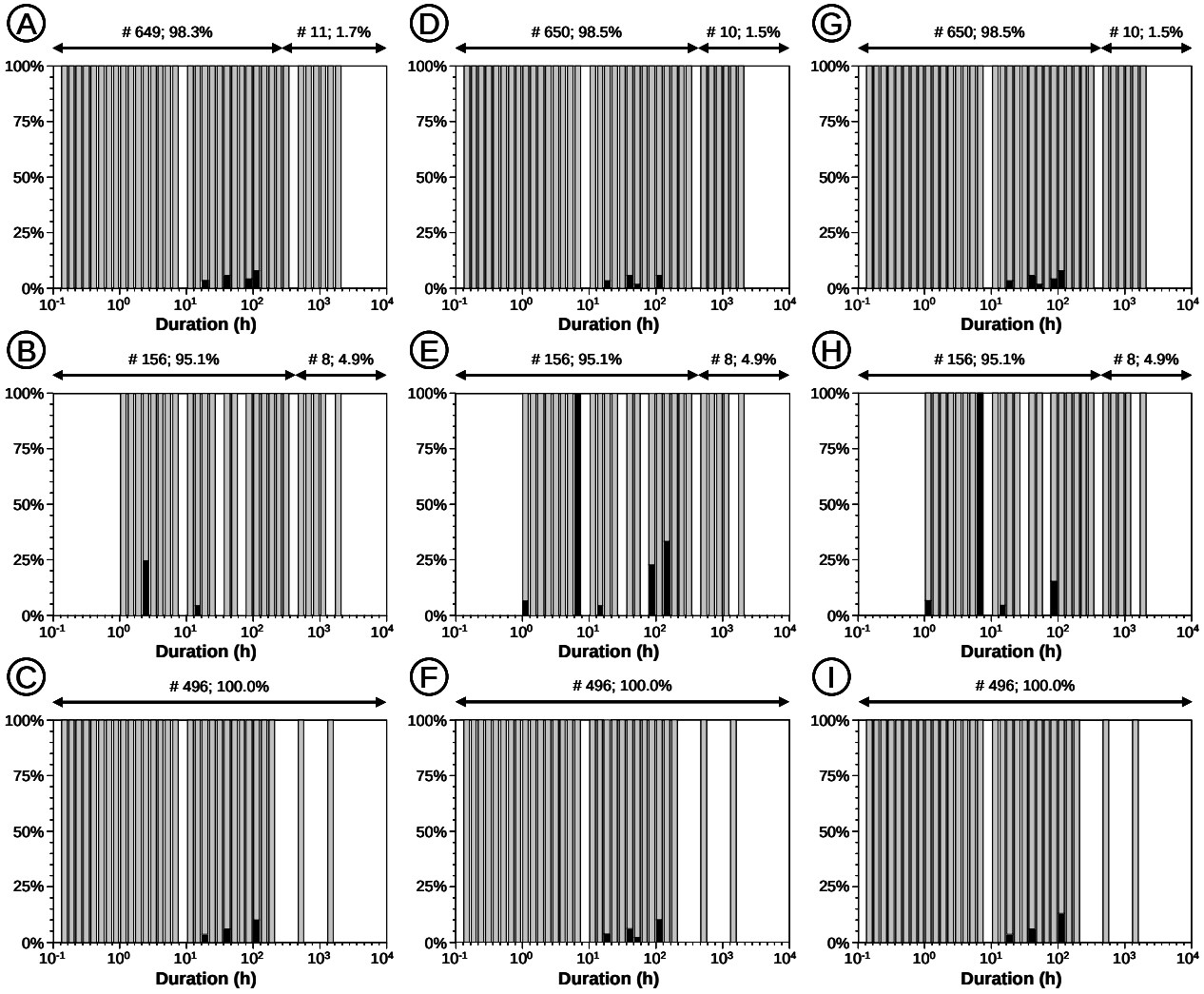
A
649; 98.3%
11; 1.7%
B
156; 95.1%
8; 4.9%
C
496; 100.0%
D
650; 98.5%
10; 1.5%
E
156; 95.1%
8; 4.9%
F
496; 100.0%
G
650; 98.5%
10; 1.5%
H
156; 95.1%
8; 4.9%
I
496; 100.0%
100%
75%
50%
25%
0%
Duration (h)

Figure 7

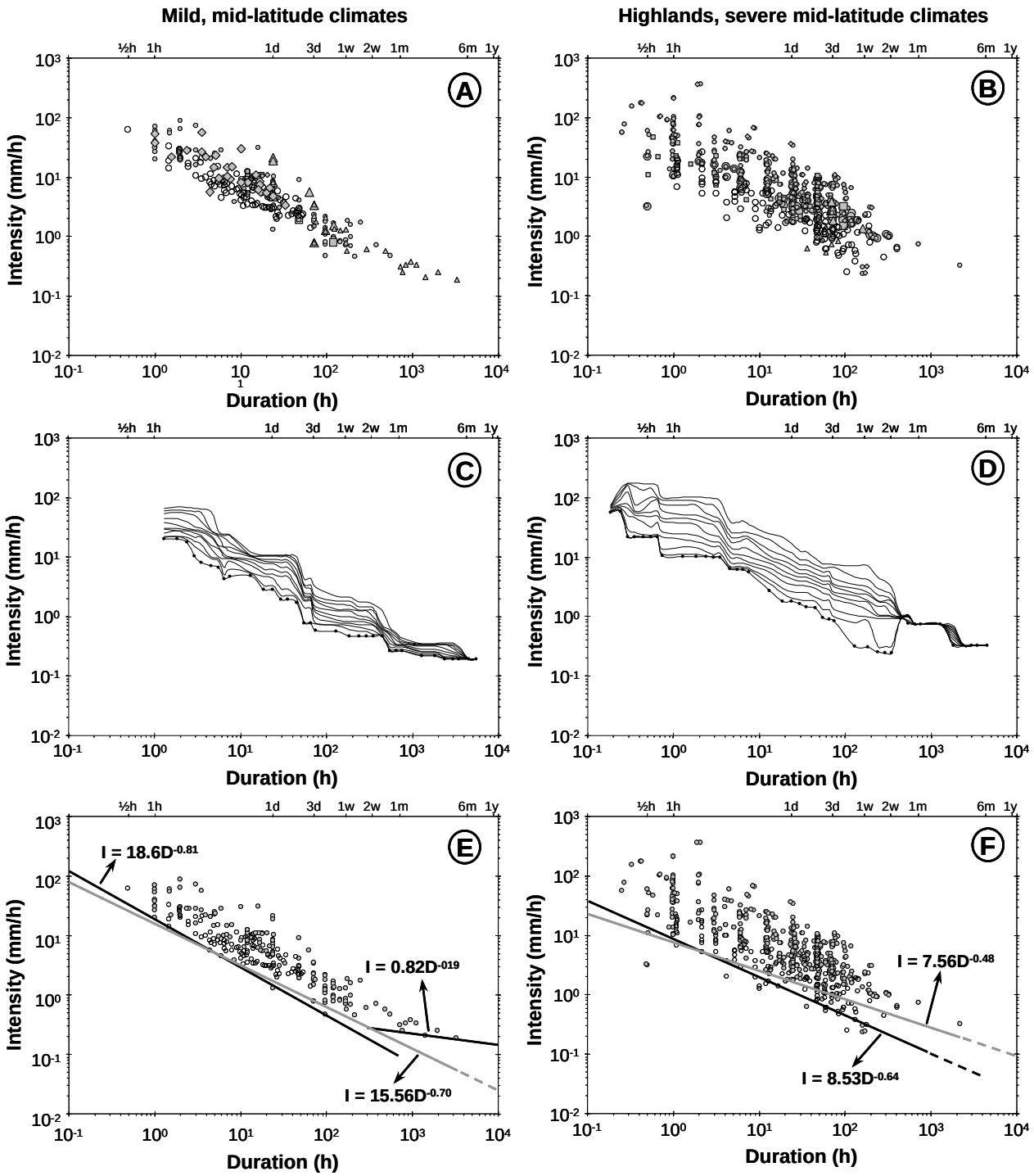
Mild, mid-latitude climates
Highlands, severe mid-latitude climates
½h 1h 1d 3d 1w 2w 1m 6m 1y
A
B
C
D
E
F
Intensity (mm/h)
Duration (h)
I = 18.6D-0.81
I = 0.82D-019
I = 15.56D-0.70
I = 7.56D-0.48
I = 8.53D-0.64

Figure 8

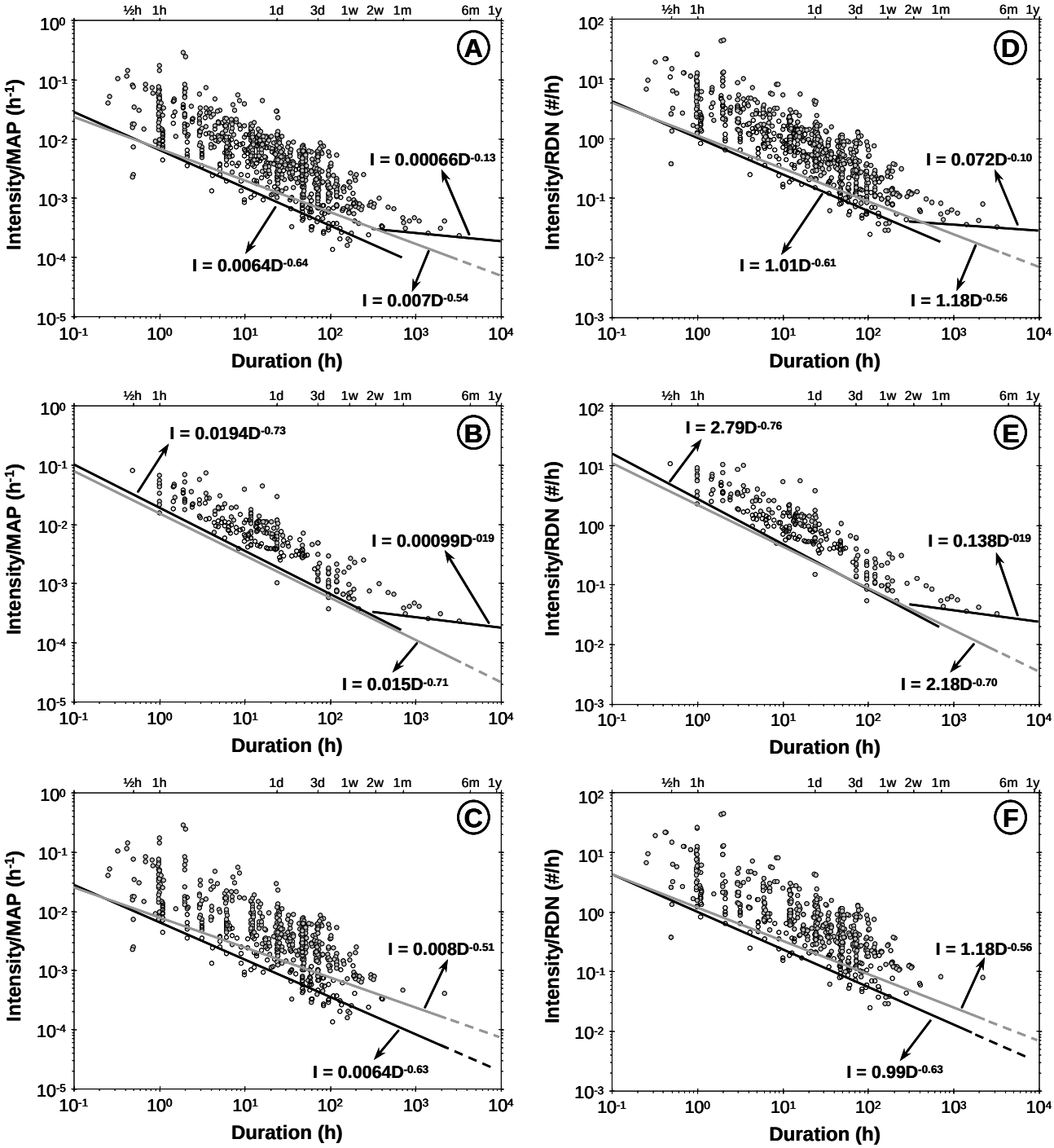
A
I = 0.00066D-0.13
I = 0.0064D-0.64
I = 0.007D-0.54
B
I = 0.0194D-0.73
I = 0.00099D-019
I = 0.015D-0.71
C
I = 0.008D-0.51
I = 0.0064D-0.63
D
I = 0.072D-0.10
I = 1.01D-0.61
I = 1.18D-0.56
E
I = 2.79D-0.76
I = 0.138D-019
I = 2.18D-0.70
F
I = 1.18D-0.56
I = 0.99D-0.63
½h 1h 1d 3d 1w 2w 1m 6m 1y
Intensity/MAP (h-1)
Intensity/RDN (#/h)
Duration (h)

Figure 9

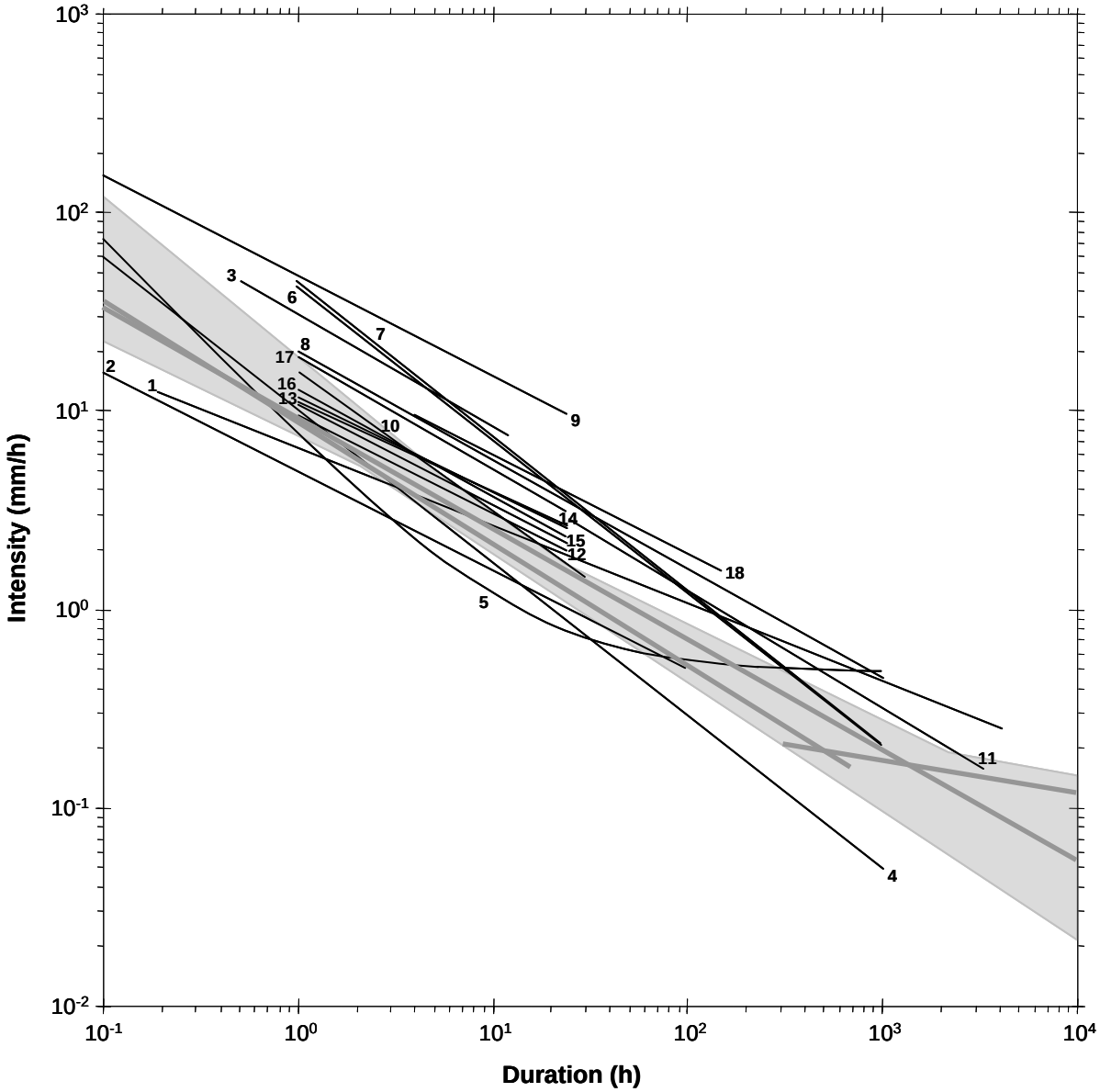
Intensity (mm/h)
Duration (h)
10^3
10^2
10^1
10^0
10^{-1}
10^{-2}
10^{-1}
10^0
10^1
10^2
10^3
10^4
1
2
3
4
5
6
7
8
9
10
11
12
13
14
15
16
17
18

Figure 10